Carbon Letters (2021) 31:557–580
https://doi.org/10.1007/s42823-021-00264-z

Online ISSN 2233-4998
Print ISSN 1976-4251

REVIEW

Carbon substrates: a review on fabrication, properties and applications

M. Ramesh[1] · L. Rajeshkumar[2] · R. Bhoopathi[3]

Received: 8 February 2021 / Revised: 5 June 2021 / Accepted: 8 June 2021 / Published online: 16 June 2021

Abstract
Carbon lives along with us in our daily life and has a vital role to play. It is present in the air and within all living organisms. Due to its handheld advantage in nano-properties that are utilized in many applications, carbon substrates came under limelight during the recent decades. Carbon substrates are most widely used in cancer detection, catalysis, bio-sensing, adsorption, drug delivery, carbon capture, hydrogen storage, and energy. Alongside, composite materials with carbon as an additive are also developing rapidly in applications like infrastructures, automobile, health care, consumer goods, etc. which became an integral chunk of our life. In this paper different types of carbon substrates and its applications, properties of the substrates were reviewed. The applications and methods of synthesis of carbon substrates are also dealt with a broad perspective.

Keywords Carbon substrates · Carbon precursor · Graphite · Graphene · Carbon nano-tubes · Hornbeam leaves

1 Introduction

Significant recent developments in the field of nanotechnology have been achieved in the last few years, especially in the fabrication of carbon substrates with a wide range of applications. The availability of carbon in abundance is the key to its presence in our lives. Carbon is contained in air and all living organisms. Alongside, composite materials with carbon as an additive are also developing rapidly in several industrial applications and play a vital role in our daily life due to its attractive attributes [1]. Carbon substrates have different characteristics, such as high elasticity, high thermal conductivity, low density, and chemical inertia, etc. These materials have played an important part in nanotechnology, electronics, optic-related applications and few other materials-oriented areas because of these fascinating properties [2]. High soluble materials could be obtained from the carbon substrates through surface functionalization and those functionalized materials were tailored and made compatible with biological systems through active molecules. Surface functionalization allows different molecules or antigens to be adsorbed or attached, which can further utilized to enhance the immune recognition or therapy effect through cell population appropriation.

Such a wide variety of materials allows various possibilities of getting different electrical, electronics, optical or mechanical properties. Various types of carbon substrates, applications, origin and their difference with other substrates according to their behaviour are dealt in this review. Some of the elements dealt here are graphite, molybdenum disulphide, graphene, graphene oxide (GO), carbon nano-tubes (CNTs), carbon nano-fibers (CNFs) and hornbeam leaves. Few central applications that pave way for newer industrial purposes, analysis of energy-efficient resources and techniques available to manufacture carbon substrates are discussed in detail in this article.

✉ M. Ramesh
mramesh97@gmail.com

1 Department of Mechanical Engineering, KIT-Kalaignarkarunanidhi Institute of Technology, Coimbatore, Tamil Nadu, India

2 Department of Mechanical Engineering, KPR Institute of Engineering and Technology, Coimbatore, Tamil Nadu, India

3 Department of Mechanical Engineering, Sri Sairam Engineering College, Chennai, Tamil Nadu, India

2 Carbon substrates

2.1 Carbon nano-tubes

CNTs are mostly applied, due to their high surface areas and appreciable physico-mechanical properties, in environmental pollution preventionand treatment, structural–functional integrated composites, energy conversion, and storage [3, 4]. During the initial stages, CNT powders were dispersed into matrix materials such as ceramics, resins and metals as nano- or micro-scale fillers for utilizing them in enhancing the conductive and mechanical performance of the substrates. Nevertheless, there are two common disadvantages in using CNTs: first is the presence of strong Van Der Waals forces in CNTs which makes them to entwine with one another resulting in agglomeration of formation of cable-like structure. Hence homogenous dispersion of CNTs into the matrix is largely impossible. Second is the increase in matrix viscosity due to difficulty in addition of CNTs into the matrix. This results in a constraint to produce the composite material with well-governed orientation. These are the reasons for the development of some novel assembly techniques, using CNT films, fibers, aerogels and 3D foams, to fabricate CNTs on macro-scale [5–7]. When these CNT macro-structures are used in the manufacturing of composites which contain governed orientation and dense CNT constituent, the resulting composite undoubtedly possesses all appreciable properties of monolithic CNTs. Table 1 enlists the enhancement of various properties and probable application areas of the composites when CNTs were used as reinforcements.

CNT films are widely used in warranted applications like air filtration and energy storage devices amongst all macro-architectures. For improving the conductivity of the composite material, CNT films may be used to modify the properties of the matrix material [8]. A thin film air filtration material was developed from CNTs due to their outstanding corrosion resistance and larger specific area. When compared with the conventional/traditional materials, the developed material had 99.9% filtering efficiency when used to filter 11 nm sized iron gel particles [9]. However, impedance to their usage is that these materials easily decompose and oxidize under aerobic conditions particularly over and above the temperatures of 450 °C [10]. Few studies stated that in air surroundings at 540 °C decomposition of CNTs were initiated which made the CNTs to possess 60% residual mass and thus the applications of CNTs for high-temperature gas filtration could not be accomplished. A revolutionary concept has been built that in lieu of CNT film, a porous ZrO_2 sponge may be utilized in high-temperature applications as a filler material. But the manufacturing of sponge is time-consuming process and upon using CNT encapsulated in boron nitride nanosheets, the oxidation temperature changed to 690 °C from 550 °C [11, 12]. Since the decomposition of H_3BO_3 in the ammonia atmosphere is required at 1050 °C, this process becomes complex to be materialized as such. It is suggested that encapsulation of CNT in silicon carbide (SiC) has increased the mechanical properties and oxidation resistance of the CNT thin films [13], but its grounding demands the usage of toxic reagents such as xylene and a high temperature of 1000 °C. Thus it is highly necessary to progress towards developing a CNT material which possesses upper hand mechanical properties, ability to withstand high temperature air environments and good oxidation resistance [14]. Figure 1 shows different biomedical applications of CNTs.

2.2 Carbon precursor

Acetylene, acetates, yeast alcohol dehydrogenase, oleates, polyurethane, low-density polyethylene, and nitro-phenol are some of the sources of carbon that were utilized for producing magnetic nano-structures based on carbon [15–18]. The novelty of combining carbon-based material with magnetic nano-particle is that it could be very well used as a raw material obtained from renewable biomass. This is possible when various organic residues like domestic, agricultural, and industrial biomass, which were underutilized, are used for preparation [19]. Advantages of agricultural biomass among these raw materials are: abundance in availability, feedstock linked functional groups range, low cost and as these materials were obtained from renewable sources they act as a recovered resources from wastes [20, 21]. A potential cradle for carbon sustenance is a carbonaceous material manufactured through pyrolysis of biomass, called bio-char, which is produced in an inert environment that is utilized for soil rehabilitation. Bio-char is also adept at removing pollutants and other heavy metals through adsorption from wastewater at a relatively lesser cost [22].

2.3 Graphene

Chemical vapour deposition (CVD) coating of graphene on substrates of solid metal was meticulously considered to fulfil numerous necessities such as transparent electrodes and electrical devices in recent years [63]. Regardless of abundant efforts, grain boundaries formed and minimizing defects during nucleation of grains [64] and imperfections caused during atomic transfers still endure as trials [65, 66]. In recent times, researchers made an effort to report the issues regarding the transfer imperfections (supporting polymer residue, wrinkles and cracks) and inadvertent organic adulteration by mounting target substrate with graphene.

Table 1 Property enhancement using treated CNTs and their applications

S. no	Matrix material	Bond and type of treatment	Condition for treatment	Property enhancement reported	Specific applications	Refs
1	Cynate ester	Covalent/Acid treated MWCNT	Using epoxy bridges	Flexural and impact strength, Glass transition temperature, storage modulus, adhesion between elements	Thermal interface applications, dampers and cushions	[23]
2	Epoxy	Covalent/Acid treated MWCNT	Oxidation condition	Tensile, impact and flexural strength, uniform dispersion	Super capacitors and shielding materials	[24]
3	Epoxy	Covalent/Amino treated MWCNT	Oxidation condition	Impact strength, glass transition temperature	Thermal interface applications	[25]
4	Epoxy	Covalent/polyamidoamine dendrimer treated SWCNT	–	Tensile strength and storage modulus	Flame resistance applications, cushions and damping applications	[26]
5	Epoxy	Covalent/Silane treated MWCNT	Normal atmospheric condition	Flexural strength and modulus, thermal stability	Electrochemical biosensors and Space vehicle protection	[27]
6	Polyamide 6	Covalent/Acid and diamine treated MWCNT	Oxidation condition	All mechanical characteristics along with dispersion of CNT in matrix	Packaging applications	[28, 29]
7	Polyamide 6, 10	Covalent/4-cholrobenzoic acid treated MWCNT	Friedel craft acylation	Tensile properties and homogenous dispersion	Packaging applications	[30]
8	Polyacrylonitrile	Covalent/4-cholrobenzoic acid treated SWCNT	Fluorination	Hardness and tensile strength	Dampers and cushions	[31]
9	Poly(p-phenylene)benzobisoxazole	Covalent/Oligo hydroxiamide treated MWCNT	Normal atmospheric condition	Tensile strength and modulus	Packaging and damping applications	[32, 33]
10	Polycarbonate	Covalent/hydrogen peroxide treated MWCNT	Oxidation followed by freeze drying	Electrical conductivity	High power electronics	[34]
11	Polycaprolactone (PCL)	Covalent/Acid treated MWCNT	Normal atmospheric condition	Storage modulus and uniform dispersion	Electrochemical biosensors and Space vehicle protection	[35]
12	Polyethylene oxide	Covalent/acid treated MWCNT	Phenoxy grafting	Storage modulus, tensile strength, yield stress and toughness	Flame resistance applications, damping applications and microwave shielding	[36, 37]
13	Polyethylene terephthalate	Covalent/Benzyl and phenyl isocyanate treated MWCNT	–	Tensile modulus and strength	Packaging and damping applications	[38]
14	Polyimide	Covalent/Acid treated MWCNT	Silane grafting	Electrical conductivity	Strain sensors, flexible electronics	[39]
15	PLA	Covalent/Acid and hydroxyl treated MWCNT	Oxidation treatment	Reduced thermal depolymerisation and enhances homogenous dispersion	Flame resistance applications	[40, 41]
16	Polymethylmethacrylate	Covalent/Amide treated CNT	Normal atmospheric condition	Thermal stability, electrical conductivity, and storage modulus	Thermal interface applications	[42]
17	Polypropylene	Covalent/Amine treated PP-graphene-MA grafted over MWCNT	Grafting polymerization	All mechanical properties	Space vehicle protection	[43, 44]

Table 1 (continued)

S. no	Matrix material	Bond and type of treatment	Condition for treatment	Property enhancement reported	Specific applications	Refs
18	Polystyrene	Covalent/4-vinyl benzyl chloride treated MWCNT	Oxidation reaction	Mechanical properties and thermal stability	Electrochemical biosensors and space vehicle protection	[45, 46]
19	Polyurethane	Covalent/Hydroxyl treated SWCNT	Grafting polymerization	Young's modulus and uniform dispersion	Cushions, packaging, strain sensors	[47]
20	Polyvinyl alcohol	Covalent/Ester treated SWCNT	Esterification	Tensile strength and homogenous dispersion	Packaging and damping applications	[48]
21	Vinyl ester	Covalent/Acid treatment of MWCNT with plaster of paris (POP) bonded amine elements	Normal atmospheric condition	Electrical conductivity, incorporation of POP rendered better dispersion	Microwave shielding and general shielding materials	[49]
22	Epoxy	Non-covalent/2-amino ethanol-treated MWCNT	Alkali environment	Storage modulus and electrical conductivity	Flame resistance applications and microwave shielding	[50, 51]
23	Polyamide 6	Non-covalent/Sodium-aminohexanoic acid treated MWCNT	Oxidation treatment	Electrical conductivity	Strain sensors, flexible electronics	[52]
24	Epoxy	Non-covalent/Titanium doped MWCNT	Normal atmospheric condition	Elastic modulus	Packaging and damping applications	[53]
25	Polycarbonate	Non-covalent/P3HT-graphene-PCL treated MWCNT	Normal atmospheric condition	Electrical and mechanical properties	Microwave shielding, flexible electronics	[54]
26	Polyamide 6 & Acrylobutadienestyrene	Non-covalent/Sodium-aminohexanoic acid treated MWCNT	–	Electrical conductivity	Microwave shielding	[55]
27	PMMA	Non-covalent/P3HT-graphene-PMMA treated SWCNT	Oxidation treatment	Tensile strength, Young's modulus and high elongation at break	Packaging and damping applications	[56, 57]
28	Polypropylene fumarate	Non-covalent/surfactant treated CNT	–	Compressive modulus and yield strength	Cushioning applications	[58]
29	Polystyrene	Non-covalent/P3HT-block-PS copolymer treated SWCNT and MWCNT	Oxidation treatment	Decrease in percolation threshold	Electromagnetic interference shielding	[59]
30	Polystyrene	Non-covalent/Pyrene assisted styrene treated MWCNT	Maleic anhydride block polymerization	Electrical conductivity	Strain sensors, flexible electronics	[60]
31	Sylgard 184 silicone	Covalent/7-octenyltrichlorosilane (7OTCS) and n-octyltrichlorosilane (nOTCS) treated MWCNT	Functional polymerization	Young's modulus and uniform dispersion	Biomedical applications	[61, 62]

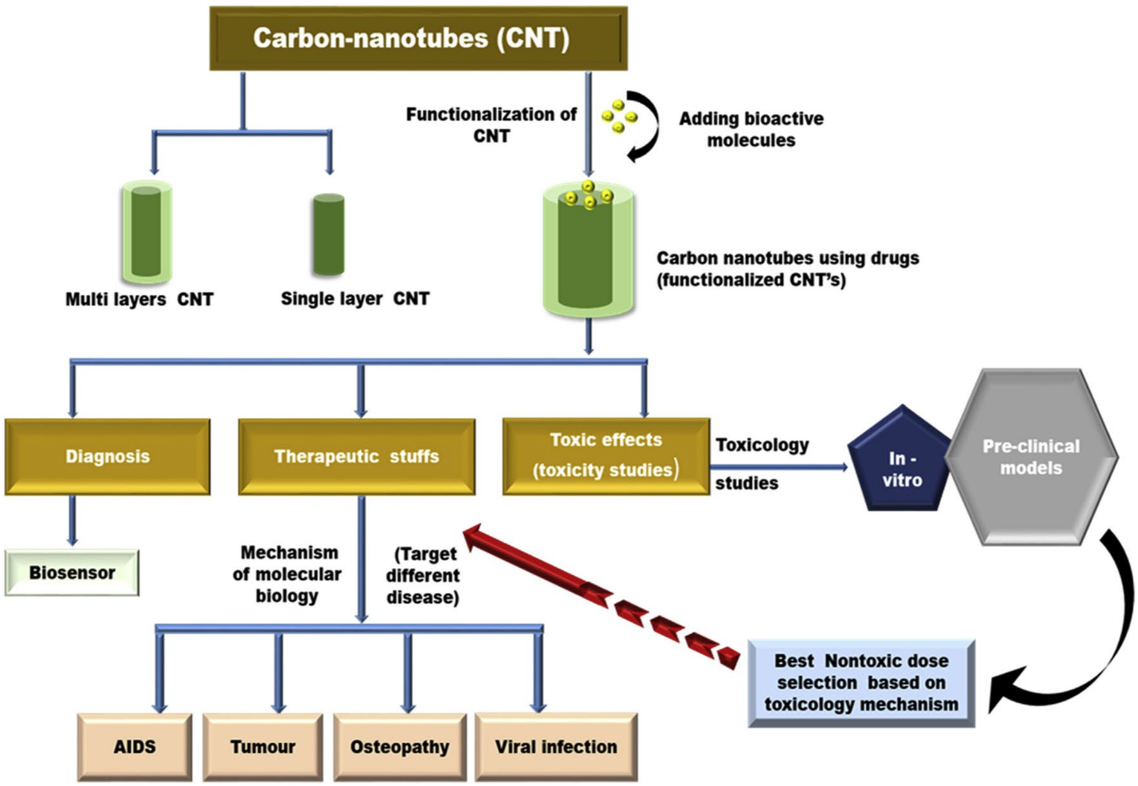

Fig. 1 Biomedical applications of CNTs [2]

Earlier researches on the development of transfer-free graphene also has the finding of appropriate carbon pre-cursor, growth of graphene over the metal substrate through the solid carbon source diffusion without the involvement of catalyst depressing the growth temperature. Yet, crystallinity and the exposure of cultivated graphene remain unparalleled with the graphene cultivated on the metal substrate through a thick foil or pre-deposited thin film of metal along with catalytic action [67].

One of the noteworthy efforts for cultivating graphene could be through the use of metal vapour as catalyst on the substrate metallic element. Few experimenters tried to grow graphene initially from the off-site evaporation of floating copper from copper foil to produce decaying carbon from which the graphene layers could be made to grow directly on oxide substrates by means of remote catalytic process [68]. In later times, some other authors stated the ease of graphene growth on amorphous substrate with copper vapour assistance by the abundant feed of copper vapour. Nevertheless, graphene was obtained with a large crystalline index from the former case was on par with the latter case but the only lacuna is the coverage of surface area of grown graphene on the metal substrate. Though the cultivation of graphene on the metal substrate using catalyst was easier, very less understanding of the mechanism of graphene growth in terms of metal catalyst vapour pressure and the substrate-specific location at which the growth and reaction took place rendered lesser surface area of graphene [69, 70].

For understanding the graphene growth arising out of vapour-phase metal catalyst that enables the direct cultivation of graphene on several substrate surfaces, precise control of the environment of graphene growth and vapour pressure of metal has to be ensured [71]. Accordingly, an MHW-CVD system with dual heating entailed with a high temperature mobile wire at a temperature of 1250 °C and another heater in the substrate bottom at a temperature of 600–700 °C in a gas controlled environmental chamber was found to work as expected because of two advantages: (i) detailed and discrete control of the PNi of metal vapour by regulating the metal catalyst temperature executed as MHW at the time of attaining individual chamber pressure control in total, and (ii) controlling the growth temperature for obtaining low defect and high area coverage of graphene independently. With these advantages, it has been efficaciously verified the thorough process of growth of graphene nano-clusters recrystallization, nucleated on a catalyst metal surface which grow and combine through monitoring of the external process parameters one after the other including T_{sub}, T_w, and wire scan speed (V_w), that concluded normality of MHW-CVD to graphene growth on NCS also. Thermal performance, life, and durability of the materials used in electronic devices have been considered vital due to their miniaturization and integration. Thermally conductive polymer matrix composites reinforced with graphene or filled with thermally good graphene has a great potential to be used in electronic applications which could dissipate the heat produced in photonic, electronic, and optoelectronic systems with ease. Many studies focussed in analysing the performance of thermally conductive graphene-containing polymer composites and their influence over other properties of such composites [72–76]. Table 2 lists the thermal conductivity values and the increase of thermal conductivity of the composite materials containing graphene.

2.4 Graphite

Graphite is present in commercial lithium-ion batteries (LIBs) as dominant-negative electrode. The major constraint in large-scale usage of LIBs in energy storage systems and electric vehicles is that it has an unsatisfactory performance and very limited lifecycle. In view of obtaining an extraordinary performance graphite anode, surface modification that includes surface decoration and surface coating are the key strategies and these changes may cater the hostile need of large-scale utilization and longer lifecycle [81, 82]. Accommodating the electrode volume changes, shielding the electrodes against corrosion and impeding the electrolyte corrosion are the key functions of the interfacial decoration layer [83].

Based on the concept of lithium solid electrolyte interphase (SEI) was analysed for a long period, especially in advanced electro-chemical systems on the graphite surface. The active material surface containing ultra-thin functional film cannot have much importance. Mostly, SEI is a nano-sized layer developed naturally superficially on electrode through electrolyte components decomposition. Texture, stability, composition and conductivity of SEI film perform critical roles on overall electro-chemical performances for graphite anodes [84]. Over 10% of the graphite particles changes at the time of extraction and insertion of lithium is being reported. Appreciable flexibility and ductility of SEI film is necessary for it to remain undamaged during the volume change occurrence. Nevertheless, many inorganic salts like LiF and Li_2CO contained in SEI film increases its brittle nature and hence coping to volume change of graphite particles is a crucial task for the film. This results in loss of lithium inventory in the cell, as the SEI film is influenced by continuous growth of mechanical crack and constant redisposition of SEI film. This is the root cause of commercial LIBs, for capacity-fading when deep charge–discharge cycles take place [85, 86].

It becomes very much necessary to form a tough and flexible SEI film to evade the lithium depletion and change of volume of graphite particles during lithium extraction and insertion. Nevertheless, rigorous attempts have been made to optimize the electrolyte by incorporating the film-forming electrolyte additives. But this strategy is least operative which increases the flexibility of SEI. In the interim, during prolonged cycles, an appreciable resistance is noted because of precipitation of unnecessary passivation species on graphite surface. Physical surface coating or alteration such as polymeric coatings [87], conductive Ag or Ni metals [88], inert metal oxide coatings with Al_2O_3 or ZrO_2 and carbon layer coatings are some of the salient strategies to enhance the life of graphite anode. Many physical coating materials may not involve in the formation of SEI layer, since most of them are electro-chemically inert, as per studies. During cell operation, another problem of mechanical mismatch between the coating layer and graphite substrate arises [89]. Electro-active SEI template materials are used to improve the mechanics of SEI film which is a sporadic study performed in contrast to the previous fact. The accumulation of a flexible SEI layer to reduce the lithium consumption by commendably housing the volume change of the graphite is highly important to develop LIBs of appreciable durability and reliability. A new method to construct elastic and robust SEI on graphite surface through in-situ polymerization technique of sodium maleate on graphite powder particles as substrate has been projected earlier [90].

The unsaturated carbon bond in maleate substrate was converted into radical thus accommodating an electron and brought polymerization reaction in between monomer and maleate. The polymeric skeleton grown upon in-situ conditions turns into a SEI film reinforcing grid, thus rendering enhanced flexibility and strength of the electrolytic interphase film. The delicate scheme and parameter of the interphase film stimulate the change in volume of graphite particles from the extraction and insertion of lithium ions. Yet, the influence of the type of carbon bond formation over the SEI film that was grown by in-situ method with graphite anode as a substrate has not been explored to a larger extent. Undoubtedly an exhaustive study on the subject of the variant of carbon is of prodigiousworthto choose a nuptial SEI substrate over which the high performance graphite anode grows [91, 92].

Graphite is a capable material with applications such as field emission, solar cells, catalysis, batteries, membranes, dry lubricants and fuel cells has a two-dimensional (2D) layered structure like graphene [93]. Current research emphasizes the quest for the optimum morphology to uphold the superior along with unique characteristics. It is described that nano-particles with visible edges unveiled the absence of superior and unique properties in bulk material equivalent [94, 95]. Some metals, carbon, silicon, and sapphire are preferable nominees for utilizing as reference materials for making few exciting 2D materials [96]. Amongst these, carbon

Table 2 Thermal properties of graphene based composites

S. no	Sample composition with graphene wt. %	Orientation of graphene	Surface treatment technique	Fabrication method	Thermal conductivity (W/mK)	Increase in thermal conductivity (%)	Refs
1	Pyrene-end polyglycidyl methacrylate-graphene nano-sheet/epoxy composite with 3.8 wt. % of graphene	Random	Non-covalent treatment	In-situ polymerization	1.92	226	[63]
2	Polyvinylidenefluoride)/functionalized graphene sheets/ nano-diamond composites with 45 wt. % of graphene	Random	–	Solution mixing	45.2	1.23	[64]
3	Alumina incorporated graphene nano-platelets with 12 wt. % of graphene	Random	Alumina coated	Solution mixing	1.51	57	[65]
4	Graphene nanoplatelets in epoxy composites with 5 wt. % of graphene	Random	–	Solution mixing	0.591	5	[66, 67]
5	Graphene and silicone rubber with 0.72 wt. % of graphene	Random	Covalent treatment	Mechanical blending	0.31	70	[68]
6	Graphene nanoplatelets reinforced in silicone with 16 wt. % of graphene	Random	–	In-situ polymerization	-2.62	50	[69]
7	PA6 and graphene in graphene oxide with 10 wt. %	Random	Non-covalent treatment	In-situ polymerization	2.16	57	[70]
8	1-allyl-methylimidazolium chloride ionic liquid modified graphene/polyurethane composites with 0.61 wt. % of graphene	Random	Non-covalent treatment	In-situ polymerization	0.31	57	[71]
9	Graphene nanoplatelets/polyphenylenesulfide composite with 38 wt. % of graphene	Random	Covalent treatment	Melt mixing	4.42	50	[72]
10	Graphene nanoplatelets/polybutylene terephthalate composite with 20 wt. % of graphene	Random	–	In-situ polymerization	2	61.2	[73]
11	Reduced graphene oxide/thermoplastic polyurethane with 1.04 wt. % of graphene	Segregated structure	Covalent treatment	In-situ polymerization	0.81	290	[74]

Table 2 (continued)

S. no	Sample composition with graphene wt. %	Orientation of graphene	Surface treatment technique	Fabrication method	Thermal conductivity (W/mK)	Increase in thermal conductivity (%)	Refs
12	PA6 reinforced graphene foam composites with 2 wt. % of graphene	3D chemical structure	–	Solution mixing	0.85	151	[75]
13	Vertically aligned graphene film/polydimethylsiloxane composites with 93 wt. % of graphene	Linear orientation	Non-covalent treatment	In-situ polymerization	615	3332	[77]
14	Octadecanol reinforced graphene composites with 12 wt. % of graphene	3D chemical structure	Covalent treatment	Mechanical blending	5.95	218	[78]
15	Nano-fibrillated cellulose/epoxy composites with 1 wt. % of graphene	Linear orientation	–	In-situ polymerization	13	911	[79]
16	Graphene nanoplatelets/polyvinylideneuoride composites with 10 wt. % graphene	Segregated structure	Non-covalent treatment	In-situ polymerization	1.51	68	[80]

substrates are habitually used to produce MoS_2 structures for numerous applications. Researchers stated that MoS_2/CNT hybrid structures can be applied for the detection of NO_2 gas [97, 98]. Validation of the probable employment of nanosheet made using graphene materials for energy storage and conversion by utilizing those materials to manufacture rechargeable LIBs possessing enhanced performance was made in many experiments [99]. Amorphous MoS_2 nanosheet arrays were consolidated on carbon cloth substrates and they were used as potential catalysts in rigorous hydrogen evolution reaction.

Various techniques have been proposed to attain well-contained MoS_2/carbon hybrid structures both physically and chemically, including solvo-thermal techniques, CVD, electrode position, sputtering, thermal pyrolysis and hydrothermal methods [100–103]. To have the uniform development of carbon/MoS_2 hybrids, solution-based techniques were found to be appropriate and highly operational but their production outcome is constrained by time-consuming and complicated processes. CVD methods were observed to be promising for directly synthesizing the MoS_2 layers on the target carbon surfaces and the precise control upon the nucleation of thin-walled multi-layered or monolayer MoS_2 on smooth or flat carbon surfaces was considered to be the key advantage [104]. Thus the quest to develop more naive strategies for producing uniform carbon/MoS_2 hybrid structures over complex structured carbon substrates is still in progress using vast experimental strategies [105].

2.5 Graphene oxide

Monolayer and few-layer graphene from the family of graphene converted into exfoliated graphite/graphene nanoplatelets (GNPs) have become the prime focus of research by many experimenters and their preparation methods and application to render enhanced performance composites were carried out [106]. Graphene oxide (GO), from which graphene is obtained, is a 2D material based on carbon comprising of various functional groups such as ketone, carboxyl, hydroxyl and epoxy along the edge and basal planes of its atomic arrangement. Bio-molecules were largely supported by GO owing to its rich π-conjugation structure, flat surface and high surface area. Besides, GO finds its applications in rendering uniform dispersion and stabilization of semiconductor nano-materials, metal oxides, and metals such as silver, platinum, zinc oxide and so on [107, 108].

Application of graphene in a variety of fields has been greatly supported by the formation of graphene-based derivative compounds like graphene-based nano-composites, GO, fluoro-graphene and graphane and these compounds could be formed by the incorporation of a functional group or proper defects into the basal plane of graphene [109]. Few experimental results portrayed that GO had less coefficient of friction compared to graphene in humid and N_2 conditions while few other studies on micro/nano-scale graphene usage displayed contrasting results that graphene exhibited less coefficient of friction than GO. It is difficult to understand the role of chemical modification and immobilization of bio-molecules on graphene due to the scarce availability of oxygenated functional groups that restricts its utilization in electro-chemical biosensors design [107]. Graphene-related materials like GO or reduced GO (rGO) possess various beneficial characteristics so that they can be readily used in nanotechnology-based devices.

GO can be found mostly in sheet form and is the most highly used derivative form of graphene. This contains oxygen functional groups along its edge and basal planes and has seen wide spectrum of biological applications due to its salient properties including better solubility in water [109]. GO is normally prepared by the oxidation of chemically treated graphite followed by its dispersion in any organic solvent or water. When GO is further reduced through electro-chemical or chemical reactions with the aid of residual oxygen atoms or fewer defects, rGO could be obtained [110]. Most of the existed GO nano-sheet-based materials were applied in the fluorescent detection systems [111]. GO and amine-modified GO-NH_2 are used as humidity sensing materials [110]. Size specific membranes can easily be obtained out of graphene owing to their chemically inert nature, better mechanical characteristics and appreciable thickness at the atomic level. Major applications of such graphene materials include their utilization in the membrane separation process and development of graphene membranes for desalination which were functionalized with nano-sized channels and pores through chemical and physical methods [112]. Graphene renders great support to surface plasma on polarization waves that were confined as graphene was characterized with permittivity and conductivity which can be fine-tuned through magneto-static or electro-static fields. This is considered to be the most significant application of graphene sheets or layers. Graphene-based waveguides, field-effect transistors, interconnects and antennas were given a strong research focus due to the high thermal conductivity, electron mobility and intrinsic strength of the graphene-based materials [113]. Such notable characteristics of GO make it as an effective initial material for fabricating cementitious composites with enhanced performance [114]. Graphene is in the current research trend due to its highly diversified properties including large electron mobility and high thermal conductivity which abundantly widen its scope of application [115, 116].

2.6 Carbon sheets based origami fold cores

Various human-made materials derived its initial form from the living organisms created by the nature [117, 118]. Few origami fold cores' geometric parameters were the derivatives of Miura-ori tessellation which can be enumerated through the association between its kinematic deformation performance and through some sequential geometric factors which are completely independent [119, 120]. Morphological and structural competencies were observed to govern most of the origami structure's applications [121]. Origami-based meta-materials, specifically ultra-light, strong, and stiff mechanical meta-materials are imparted with much importance. The frequently used structure of these meta-materials is frivolous sandwich materials with Miura-ori tessellation co-rearrangement and such materials are also termed as chevron origami fold core materials. Fold core structures with sandwich cross-sections have enlarged their capable applications in aircraft assemblies. Fold core sandwich structures are used as fuselage structures in Airbus aircrafts while VeSCo arrangement was taken into consideration by most of the German-based research organizations [122]. They are also used in preparing other aircraft structures like rudders, flaps, and spoilers [123]. Project CELPACT was initiated in European countries mainly to demonstrate the strong mechanical properties of chevron origami fold core sandwich structures. Few researchers studied the impact and quasi-static behaviour of chevron origami fold cores [124]. The intense anisotropy of in-plane mechanical behaviour of corrugated cores was possibly lessened by fold cores that are folded in two different directions [125]. Fold cores provide open channel for ventilation whereas the honeycomb structure has closed cells [126]. By strategic design for geometric parameters in the unit cell of fold cores, they may accommodate the complex curved surfaces. Sheet materials like aluminium sheet, aramid paper and composites reinforced with natural or artificial fibers were theoretically utilized for the construction of the fold cores [127–129].

Curved origami fold core comes under novel origami fold core structures. Very few studies are available on this structure and mainly focus was on the design, experimental and numerical investigation of the curved origami fold cores prepared from either plastic or metallic materials [118, 121, 130]. Alongside, only very few researches are available on the investigation of curved origami fold cores prepared from natural or synthetic fiber-reinforced composites and the analytical model to predict the performance of these structures are to be explored to a larger extent. When compared with the fold cores made of aluminium and paper, carbon fiber reinforced composite fold core materials were characterized by high strength and stiffness. It was also stated in various literature that chevron origami fold core pattern aroused from a conventional V-pattern. This pattern was developed specifically for paper or metallic materials and could not be suited for any fiber-reinforced composite materials. For fiber-reinforced composites to be used as parent material, the zig-zag crease pattern of the fold core could be converted into curved fold cores [131–133].

The main advantage of using curved-crease fold cores is that it avoids the breakage of fiber during the manufacturing of composites and loading them [134, 135]. It also minimizes the change of fiber direction abruptly. Variation of the presence of resin in a rich or meagre way was also addressed by the curved crease fold cores due to the smoother changes occurring in the cell wall of the materials. These curved-crease fold core materials possess better buckling strength and resistance when compared with chevron fold cores [136–138]. Due to the aforementioned potentialities, carbon fiber reinforced composite fold cores are currently in prime focus in terms of research [139]. Current day researches focus on developing structures that are self-folding which could be created by the action of external forces and moments thus kindling kinematic manipulations without adopting mechanical folding or unfolding. Such automatic folding of the structures is used in robotic applications, self-assembly operations and aerospace applications. Table 3 enlists the various types of external actuation forces and their processing time along with range of folding angle for different inherent fold core materials [140–143].

2.7 Carbon nano-fibers

CNFs gained increasing interest nowadays due to their noteworthy evolution in many applications of engineering and technology. Advanced composites could be manufactured by reinforcing CNFs with either natural or other synthetic fibers and these materials could be applied in numerous aircraft, military, and automobile applications. Apart from these applications, CNFs could also be employed as fuel cell catalysts, waterborne and airborne pollutants' sorbent, tissue reconstruction, and renaissance for various bio-based materials. Different applications demand different forms of CNFs: in some applications, they are required as reinforcements or as individual fibers, in some other fields, it is required as a medium for adsorption, as energy storage and conversion materials, for stable and ease of handling biomaterials and as porous membrane in mass transfer applications [144]. Apart from the material form, various target applications demand the deployment of CNFs with variety of chemical structures and surface characteristics. From all the above facts, it could be stated that the fabrication of CNF based composites has to be planned sensibly in such a way that the specific application are catered without any lacuna. CNFs can be easily produced by electro-spinning of the polymer precursor and its carbonization. By controlling some important process variables, porous CNFs with necessitated characteristics can be fabricated [145, 146].

Among different precursors, polyacrylonitrile (PAN) was frequently used in the industrial scale. This relatively low-cost polymer might render a maximum carbon yield owing to the containment of intermittent constituents that influences the tailoring of CNFs in favour of its disintegration when they were heated. PAN rendered carbon fibers exhibit

Table 3 Actuation of origami fold cores and their range

S. no	Fold core materials	Type of actuation	Time of actuation	Range of folding angle (degrees)	Refs
1	Polyethyl ethyl ketone film	Thermal force	0.01 s	0–720º	[117]
2	Polyimide film with paper board	Thermal force	0.015 s	NA	[118]
3	Titanium nitride with shape memory alloy	Thermal force	0.1 min	NA	[119]
4	Polyvinyl chloride with aluminium coated polyester	Thermal force	3 min	60º–115º	[122]
5	Polystyrene film with paperboard	Thermal force	< 1 min	0–140º	[123]
6	Paper printed with carbon and water based inks	Thermal force	9 min	NA	[124]
7	PolyN-isopropyl acrylamideco-sodium acrylate with polymethyl styrene	Thermal force	< 1 min	0–180º	[125]
8	Graphene oxide reinforced in polydiacetylene with reduced graphene oxide	Light actuated	0.05 s	60º–180º	[126]
9	Pentaerythritol tetra 3-mercapto propionate and 2-methylene-propane-1,3-dithioethylvinylether reinforced in ethylene glycol di 3-mercaptopropionate	Light actuated	900 s	60 º–180 º	[131]
10	Gallium arsenide cores	Light actuated	Very low	0–0.6 º	[133]
11	Dielectric elastomer along with polycarbonate	Electrical force	0.04 s	0–44 º	[135]
12	Terpolymer in polyvinylidene fluoride reinforced with TrFE and CTFE piezoelectric materials	Electrical force	0.01 s	NA	[136]
13	Polypyrrole films	Electrical force	5 s	25 º–31 º	[138, 139]
14	Polydimethylsiloxane	Electrical force	0.01 s	NA	[141]
15	Ecoflex	Pneumatic force	Depends on air velocity	0–360 º	[142]
16	Bovine aortic smooth muscle cells with biocompatible 3D microstructure	Biological cell	Very low	0–80 º	[143]

high mechanical, electrical, and thermal properties owing to the high amount of carbon output. Manufacturing of CNFs from PAN could be easily customized and a clear picture on the quality of CNF can be obtained by the influence of various process parameters on the properties of the final product. As the commercialization and application of nano-fibers has high scope, various researches were conducted upon the fabrication aspects of CNFs and their optimization. From such studies, various dimensional and structural aspects of CNFs such as its diameter, morphology, and structural arrangement were obtained. Yet, more explorations in terms of physicochemical characteristics of CNFs and modified thermal transfer within those nano-scale fibers have to be done by systematic experimental investigations. Another possibility of diversification in the study could be the modification of CNF precursors by mixing them with different types of additives [147, 148].

Additives were employed for two primary cause. First, to stabilize and carbonize the fibers as catalysts to reduce the thermal treatment temperature and time, for the industrial scale fabrication at low cost. Second, additives might be influential in changing the material properties like thermal, surface chemistry, electrical conductivity and mechanical properties [149]. Introduction of the additive was expected to convert the process as simple one simultaneously when the precursor was also made. It was also stated that addition of additive should be carried out like post thermal treatment which might not have much reduction in process cost. Electro-spinning of the additive modified polymer matrix was considered to be the simple and one-stop solution for the aforesaid problem [150]. Transmission electron microscopy (TEM) images of single and double-layer CNF is presented in Fig. 2 [151].

Amongst various additives of CNF, CNTs are important, because of contained graphene, it not only compromises some properties but also aids in enhancing a few of the end characteristics of fabricated material [151, 152]. Simultaneously, the mechanical characteristics of the available CNFs were assumed to be inherently better owing to their shape factor. Researches pertaining to the influence of the CNTs addition in PAN nano-fibers with respect tothermal transition process were noted [153]. Nevertheless the interaction mechanism of CNTs-polymer with reference tovarious characteristics and their effect on thermal transition process remains ambiguous even now. This unclear scenario arose due to the complex chemical composition of graphene and graphene plane transition in CNTs at the time of thermal processing [154]. It was also stated by few experimenters that the change in dimensions of CNT and the rate of homogeneity in the dispersion of CNT in polymer matrix could bring a change in transition mechanisms. Such unclear characterization at the time of their incorporation in polymer matrix gotten even more complicated during the earlier times as the purchase of materials by the experimenters were made from various vendors and the materials itself were different in nature [155, 156].

The difference of the CNT materials was not only present with respect to the various vendors but also with respect to various batches of material supplied. This forced the experimenters to carry out a complete characterization of CNT used in the experiment to have clarity in end material characteristics. Such usage of CNT as reinforcement in the polymer matrix and their prior characterization became a significant part of research and the availability of CNT commercially has also seen much growth due to high availability, price reduction and the availability of functionalized CNTs which has also amplified the applications ofCNF. Functional groups available at the peripheral walls may vary in terms of magnitudes and types and the usage of such CNTs have a significant influence upon the polymer matrix chain which aids in developing different materials with variable structural and surface properties to cater the precise requirements for the objective uses [157–160].

2.8 Activated carbon and carbon black

Activated carbon (AC) is a carbon-based material which is characterized with a large surface area and higher degree

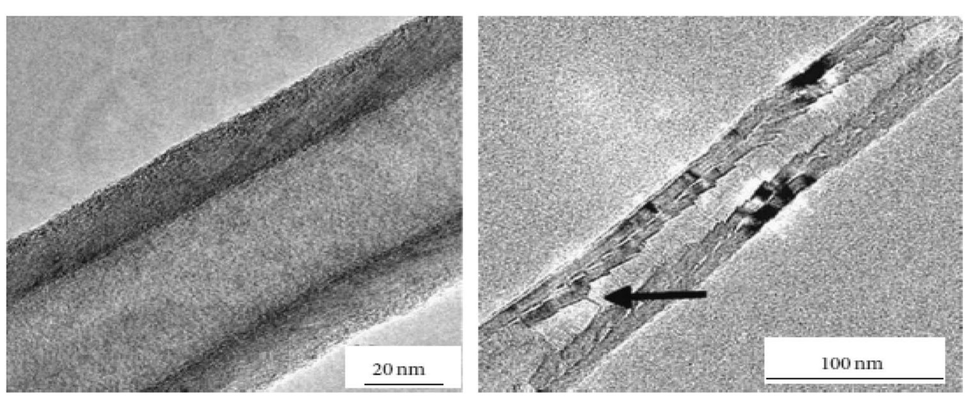

Fig. 2 TEM images of single and double layer CNF [151]

of porosity. It can also be termed as carbonaceous material with porous structure which is used in various applications including desalination and wastewater treatment and purification of air owing to its noteworthy characteristics [161]. It could also be used in various other applications pertaining to industrial scale and environmental-related applications such as separation, retrieval, modification, and removal of gas and liquid phases from different compounds. AC comprises of almost 90% of carbon while the prominent functional groups present in activated carbon including lactone, phenyl, quinine, carboxyl and carbonyl groups were responsible for contaminants absorption. AC structure consists of nitrogen, oxygen, sulphur, and hydrogen as functional groups in its chemical structure [162].

Specific adsorption characteristics of AC were due to the presence of functional groups within it, which were activated by various activation processes such as thermal and precursor purification. Applicability and performance of the activated carbon material purely depends on the choice of chemical activation agent [163]. Numerous alkaline-based chemical agents such as potassium carbonate, potassium hydroxide, calcium chloride, and sodium hydroxide, acidic chemical agents such as sulphuric acid and phosphoric acid and metal intermittent salts including zinc chloride were majorly used as activating agents for activated carbon [164]. Figure 3 depicts the activation process and chemical used for the activation of AC. Since various factors govern the activation degree of AC, numerous researchers are currently being conducted to clearly comprehend the mechanism of adsorption so that the process of adsorption can readily be employed in adsorbing the atmospheric pollutants using AC can be unveiled and developed for future purposes [165, 166].

Carbon black (CB) is manufactured by decomposing the carbon-rich ingredients in a completely controlled inert and oxygen deficit environment through partial combustion or through pyrolysis. In most of the applications, CB was used as filler reinforcement in many rubber-based composites and to enhance the overall characteristics of elastomer-based composites [167, 168]. It was found from various studies that CB filled in composites exhibited better dynamic, elastic, and enhanced mechanical characteristics along with good resilience and resistance towards scratch. Almost 92% of CB production in global basis is used in the manufacturing of tyres, especially some tyre elements including carcasses, inner layers and few other components like belts, vibration isolation devices, air springs and belts [169].

Yet, owing to top reasons like continuous non-renewable raw materials use and enhanced pressure developed from the unsustainable manufacturing methods of CB, the modification of CB and development of derivative substitution filler materials for rubber has been given the prime focus of research keeping in mind the future economy and environment concerns. Few more researches stated that CB based nanofluids exhibited enhanced IR absorption and the network formed with CB particles enhanced the fluid's thermal conductivity. Such highly thermally conductive fluids are currently employed in solar distillation and heaters which have the potential to render water vapour while the heating of working fluid is no longer necessary [170, 171]. Figure 4 depicts the transmission electron microscopic images of CB and the CB exfoliated for 20 min.

3 Fabrication processes

3.1 Pyrolysis

Pyrolysis is a thermo-chemical technique that decomposes carbon-based material in an inert atmosphere at a temperature of 400 °C and transforms them into bio-char, bio-gas and bio-oil [172–174]. It is extensively adopted and deliberated as a capable process due.

to its simplicity and low cost [175, 176]. It consists of two steps: first, removal of moisture and the second, production of bio-gas, through conduction and convection,

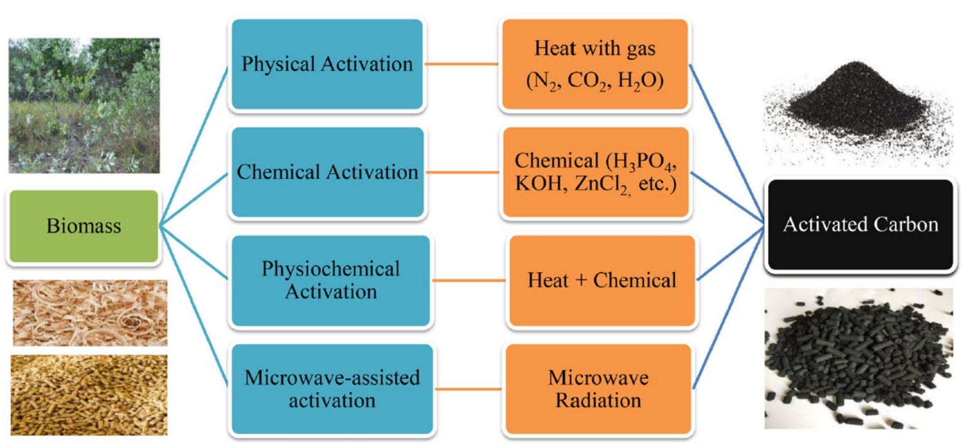

Fig. 3 Activation process and chemicals used to activate the AC [166]

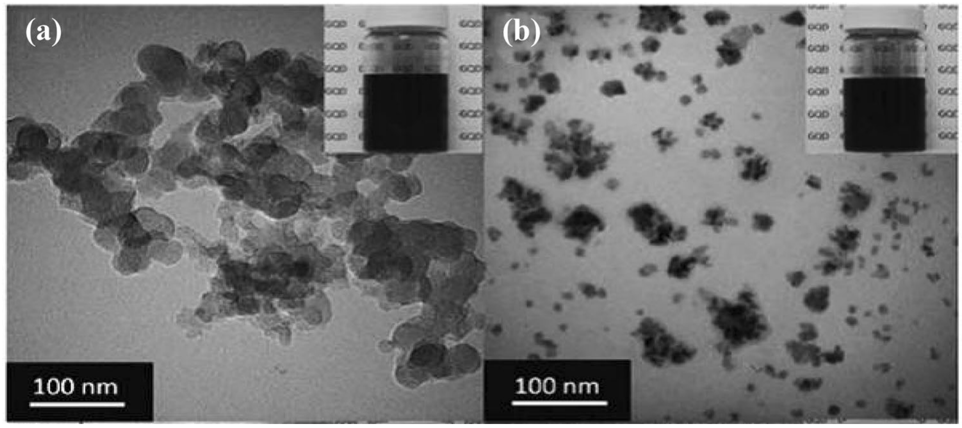

Fig. 4 TEM images of **a** CB; and **b** exfoliated CB for 20 min [170]

due to increase in temperature and further breaking down of cellulose and hemi-cellulose contents which results involatile components removal [177–179]. Volatile material removal from the biomass surface indices pores on the surface of biomass which was due to the degradation of cellulosic and hemicellulosic micro-constituents from the biomass surface during the initial stage. The combined effects of constant heat transfer and auxiliary volatilization increases the pore size thereby enhancing the carbon content during the subsequent process stages. Magnetic component integration occurs by post-coating or pre-coating pyrolysis process [180]. Figure 5 depicts the schematic setup of pyrolysis with various components in it.

3.2 Chemical co-precipitation process

Chemical co-precipitation technique is a widely used one for manufacturing nano-materials and the key motive is parting of grain growth and grain size of the product may also be obtained as an outcome due to the sluggish nuclei growth [181–183]. In this method, solute precipitation occurs, segregating it, and ultimately binds with the solution without dissolving. Solute binding marks one among the following three methods of precipitation which are surface adsorption, inclusion, and occlusion [184]. When the carrier is completely surrounded by the solute at the time of formation of crystal lattice it is called occlusion whereas during inclusion solute crystal matrix mixes partly along with the matrix of carrier crystal. Nonetheless, solute surface adsorption is superficially carried out which completely leaves the solution generating a huge surface area in the substrate [185, 186]. This technique is effectual to manufacture extremely ultrafine grains of size ranging between 5 and 8 nm and any size in this range of nano-material could be fabricated through the chemical co-precipitation technique [187].

3.3 Hydrothermal carbonization

Hydrothermal carbonization (HTC) is a well-organized technique for the manufacturing of nano-materials [174, 188, 189]. Nowadays it has concerned more about the development of multifaceted nano-sized structures with dissimilar properties. As a matter of fact, HTC technique falls back to yester-century in time with the objective of charcoal manufacturing [190]. Substantial advances of the HTC techniques were executed from the earlier time so that it transforms into a potential processing technique to convert polysaccharide complexes into solid products at different range of temperatures. The temperature range for this technique was determined to be in between 150 to 350 °C and the pressure range was in between 2 and 10 MPa with the processing time-spanning for few hours and all the parameters dependent on the end product needed along with the type of material used [191]. Usually, HTC technique water as catalyst due to its higher constant of ionization and so this process has a high rate of hydrolysis which would not assist material disintegration. As the HTC technique is a wet process, drying of raw materials becomes unnecessary which turns HTC process to be energy efficient. Features of HTC treatment techniques listed by earlier researchers were carbon content promotion in the final product, solubility improvement, complex acid–base reaction promotion, crystalline matrix melting and acceleration of solvent-carbon physio-chemical interactions [174, 192]. Few experimenters stated that HTC technique was widely employed for the manufacturing of carbonaceous nano-sphere mono dispersion from initial ingredients in a controlled environment which ensures homogenous dispersion through aromatization, condensation, dehydration and polymerization of the materials [193]. This technique promotes a high reaction rate by means of generating high oxygenated functional group which ultimately renders higher porosity that is considered to be a key factor in reactions like carbon capture, catalysis, super capacitance and adsorption.

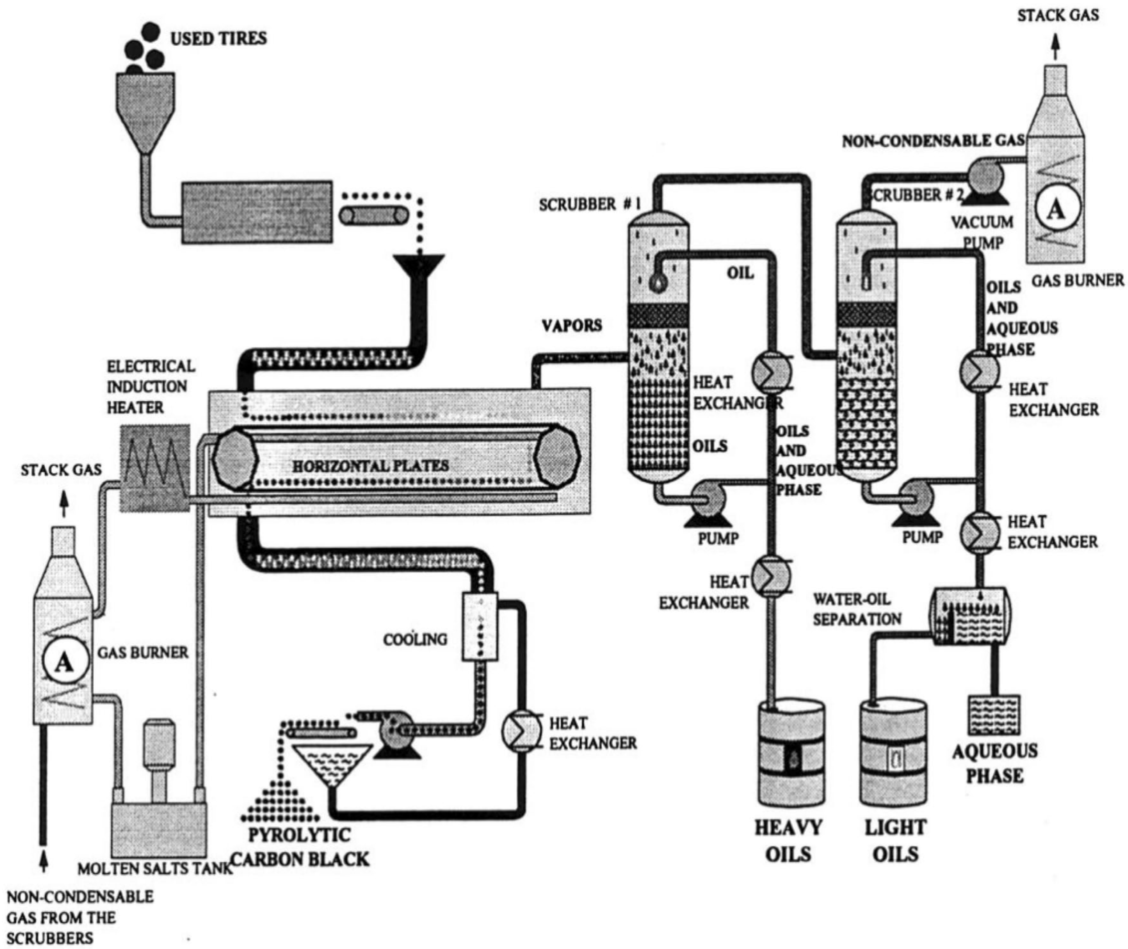

Fig. 5 Schematic setup of pyrolysis method [173]

Few experimenters stated that the porosity of the material was dependent on temperature of the process and was found to increase at 240 °C. Beyond this temperature, porosity of the material drops but the mechanical characteristics of the material improved greatly [194].

Many researchers emphasized that the role of catalysts in the HTC method was highly significant. Experiments with iron oxide nano-particles used in the HTC process rendered hollow carbonaceous spheres formation [195]. Some authors analysed that usage of iron oxide and glucose rendered magnetic nano-materials of uniform particle size for the designing of quasi-static spherical structures. These materials enabled the capability of adsorption of polycyclic aromatic hydrocarbon to be maximum [196]. A 3D porous nano-sized composite electrode was formed using the same material by some researchers. Nano-sized material produced by the above method had symmetric size and shape with a capacitance value of 259.3 F/g, surface area of the material was noted to be 1712.8 m/g and a window voltage potential of 1.8 V [197]. Nano-sized hydro-char particles incorporated in nickel–iron-based alloy was manufactured using HTC and recorded a high adsorption of lead with 99.5%. Particle size of the nano-material developed through HTC depends on precursor concentration, microwave power, time of processing, and catalyst used [198]. Figure 6 illustrates the setup used for the hydrothermal treatment method of production of CNFs.

3.4 Cold compression process

Continuous folding machines with the arrangement of cold compression were designed to manufacture chevron origami fold cores (COFC) from paper or metal sheet [124]. Few trials were performed with aluminium COFC erected with sporadically gradual stamping technique and with the aid of cold gas pressure as a novel processing method; the metallic sheets were folded into COFC [125, 199]. Researches were enormous efforts implemented few novel methods to evaluate the compression strength of the COFC sandwich structures formed from aramid papers both by numerical

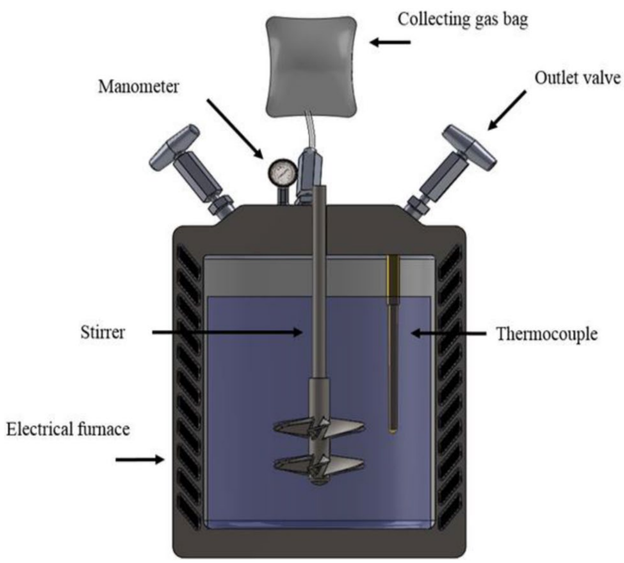

Fig. 6 Schematic setup used for HTC process [174]

simulation and experimental methods. Few other experimenters examined the failure behaviour and stiffness characteristics of aramid COFC under combined shear and compression loads [131, 200–202]. Cold compressed aramid sandwich COFC were subjected to the evaluation of combined bending and in-plane compression analysis through experiments by many authors. In addition to the above studies, aluminium COFC sandwich materials were used in experiments to determine their mechanical behaviour specifically under compression by few researchers [134, 203]. Yet, exploration of cold compressed fold core materials in terms of analytical models to evaluate the quasi-static mechanical characteristics were to be made and such lacuna was presumed to be due to the structural complexity of the sandwich fold core structures. Besides the advantageous mechanical properties, some other characteristics such as thermal and acoustic characteristicsare the inherent meritorious features of chevron origami fold core structures [204]. Table 4 encompasses various fabrication methods used to extract CNFs and their process parameters along with the energy consumed in Frigoria (F/g).

4 Characterization

Figure 7 illustrates the hierarchical photo-resist structures of micro- and nano-size fabricated by varying the height of the substrate and also the etching time. SU8 photo-resists comprising of antimony along with a minimal quantity of aluminium scrunched out of chamber of plasma masks the vicinity of SU8 photo-resists. During etching, it is

Table 4 Fabrication process and its parameters to extract CNFs

S. no	Source of raw material	Extracted CNF diameter (nm)	Fabricating method	Time of processing	Temperature	Pre- and post-treatment	Usage of cooling medium	Energy required (F/g)	Refs
1	Cellulose nanofibrill	21	Pyrolysis	Low	High	Chemical treatment/Not required	Not required	81	[205]
2	Bamboo	25	Pyrolysis	Low	High	Chemical treatment/Not required	Not required	792	[206, 207]
3	Seafood chitin	29	Pyrolysis	Low	High	Chemical treatment/Not required	Not required	111	[208]
4	Crab shell	71	Pyrolysis	Low	High	Chemical treatment/Not required	Not required	128	[209]
5	Sawdust	102	Electrospinning	High	Less	Chemical treatment/Carbonization	Solvent solution	90	[210, 211]
6	Lignin	99	Electrospinning	High	Less	Chemical treatment/Carbonization	Polymer solution	66	[212]
7	Cellulose	200	Ultrasonication	Low	Less	Not required/Carbonization	Solvent solution	146	[213]
8	Natural fungus	630	Hydrothermal method	High	Less	Chemical treatment/Not required	Polymer solution	175	[214]

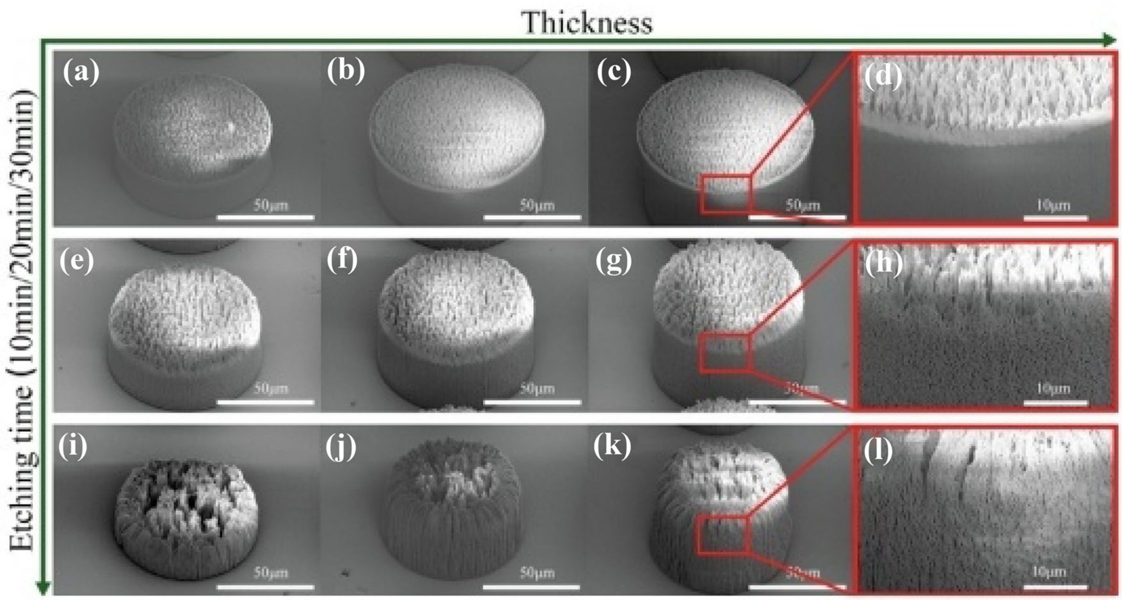

Fig. 7 **a**–**c**, **e**–**g**, **i**–**k** SEM images of the photo-resist structures with varying height and etching time; **d**, **h**, **l** magnified views of (**c**, **g**, **k**) [215]

perhaps,substrate iron will be a mask of the photo-resist. Additionally, the travelling direction of oxygen plasma etch induces nano-sized wires upon the peripheral boundaries of photo-resist over the cylindrical structure during etching [214, 215]. Figure 7a, b, c, e, f, g, i, j and k depicts that the increase in etching time using oxygen plasma reduced the cylindrical structure diameter and when the depth of photo-resist nano-wire etching increases, thinning of nano-wire surface also occurred. It could also be noted that the edge of photo-resist nano-wire was distorted owing to uninterrupted etching, resulting in a ring-shaped structure as shown in Fig. 7i–k. Additionally, as the time of etching increased, the micro/nano-structures of the photo-resist surface turned into flurry, and also enlargement of side walls pores occurred, as shown in Fig. 7d, h and l [215–217].

The representative Fig. 8 denotes of MnO_2/carbon micro- and nano-structures manufactured through mechanisms like electro-chemical deposition and carbonization. Figure 8a–c illustrates the photo-resistant structures of MnO_2 materials that were fabricated in various heights and their time of etching was maintained as 10, 20, and 30 min in order. Figure 8a, d and e denotes the deposition of MnO_2 particles over the substrates when they were exposed to an etching time of 5 min which was lesser among all other durations. When the exposure time is increased, the deposited MnO_2 particles were of larger particles as seen in Fig. 8b and c. The XPS spectrum of MnO_2 structures, depicted in Fig. 8f, exhibits two major peaks at two values of binding energy such as 642.6 and 653.9 eV. The peak values were analogous to the earlier MnO_2 values thus depicting the dominant presence of Mn^{4+} [215–218].

5 Applications

Production of magnetic property-rich carbon substrates from the abundantly available agricultural waste may pave way for the effective utilization of wastes. In addition to the utilization, harmful gases liberated from those wastes were also reduced when the wastes are reused properly [219]. Though the nano-materials deal with the environmental hazards effortlessly, their disposal effects and exposing to the environments pose threat towards the environment and health [220]. Owing to their ultra-fine sizes, their mixture into the stream of wastes may end up damaging human health and the life of sea species. Nevertheless, such magnetic property-rich nano-materials could be recovered with the help of a magnetic field which makes the technology more efficient and safer. Few experimenters removed the arsenic contaminates from water using an innovative mesoporous magnetic encapsulated carbon while the thiazole fungicides were effectively absorbed by the graphene-based magnetic nano-composites from water [221, 222]. Many organic compounds like chloro-benzene, phenol, dyes, and chloroform can be absorbed from water by using the enhanced absorption potential of magnetic activated carbon and these elements need not be separated from water [223]. Many experimenters demonstrated that gases like methane, nitrogen and carbon dioxide can be absorbed by carbon nano-materials doped with iron oxide nano-particles and polypyrrole. This worked perfectly even under variations of pressures [224]. Separation capability and absorption using carbon nano-particles to adsorb and separate heavy metal ions from water are shown in Fig. 9.

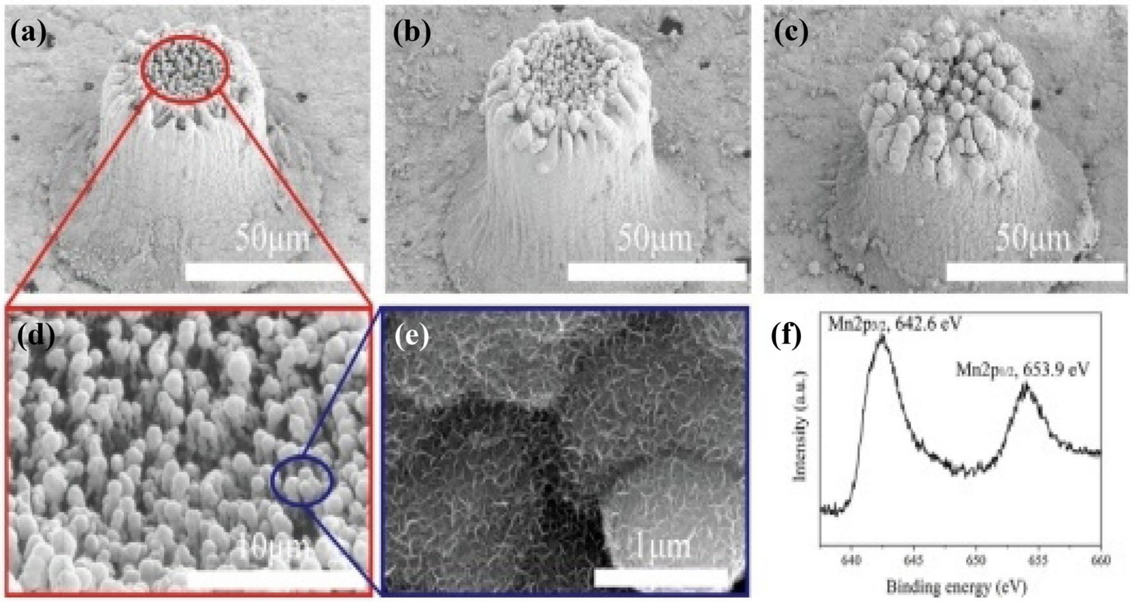

Fig. 8 **a**–**c** SEM micrograph of MnO_2/carbon structures with varying deposition rates, **d** magnified top surface of the material (**a**); **e** magnified MnO_2 nanostructure from (**d**); **f** XPS curves of the material [215]

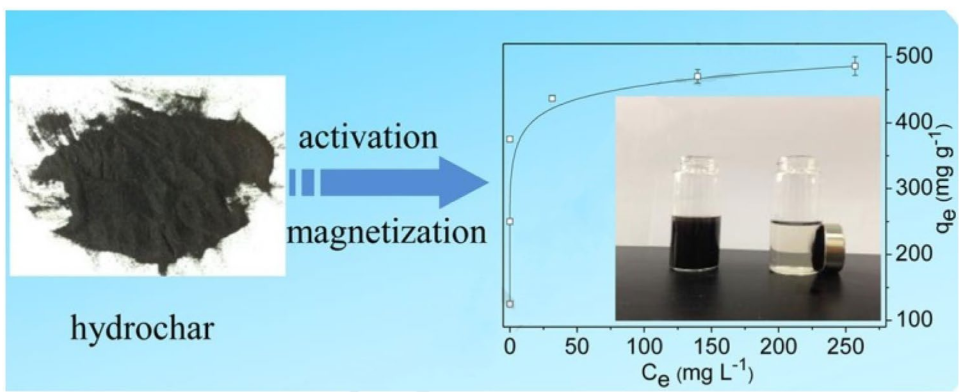

Fig. 9 Adsorption phenomenon using carbon nano-particles [223]

An effectual completion of 5000 lifecycles with almost 95% retention of capacitance was done by carbon nano-wires that possess a power density of 1.2 kW/kg, specific capacitance of 259 F/g and a maximum energy density of 30Wh/kg because of their good electrical durability [225, 226] which performed in lithium-ion batteries also as an anode. High surface area, lower cost, super electro-magnetic properties, and non-toxic nature are some of the advantages of carbon substrate materials apart from high energy capacity [227, 228] which approve their usage in energy storage applications. Hydrogen storage can also be done using carbon substrates as experiments focus on manufacturing flower-like structures with magnetic microspheres utilizing L-cysteine [229].

Nano-sized materials are highly used in health care applications potentially for more than three decades. An important problem in the usage of orthodox nano-materials is making them work in the areas of target in the human body. The induction of magnetic nano-particles expedites management to explicit are as by the meek practice of a magnetic field all through treatment process, trailed by delivery and then by capable removal of the field [227–229]. One well-established area is the visualization of musculoskeletal structure along with soft tissue using magnetic resonance imaging (MRI) technique that utilizes differently natured materials like iron oxide-based nano-material for obtaining high-quality images [230]. Due to higher retention time and higher permeability, these nano-particles can detect tumours efficiently (Fig. 10). Some other researches focus on using the nano-materials as drug carriers and for gene therapy in which the nano-magnetic transfection into the cells is made non-virally [211–214]. Using nano-materials, effective

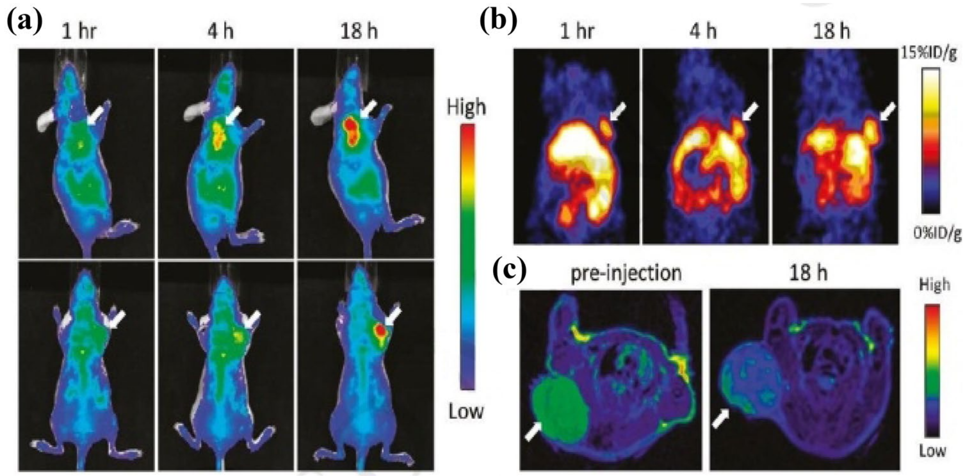

Fig. 10 MRI images of detection of the tumour through magnetic particles [217]

cytotoxic drug delivery has been stated on various animals [214, 215, 220]. Improvement in novel nano-material carrier systems is the key area of current researchers and drug delivery can be materialized by the application of surface engineering techniques. Alongside the field of bio-sensor and bio-chips using nano-material are also under development [231].

6 Conclusion

In this article, a complete outline about the properties and manufacturing methods of newer carbon substrates were discussed in detail. Details of carbon substrates used to produce lightweight fiber reinforced plastics and other areas where reduction of weight is needed without compromising the strength were also enumerated. Extraction methods, developments and other supportive data of carbon substrates like graphite, molybdenum disulphides, hornbeam leaves, CNTs, AC, CB and CNFs were dealt in detail. These materials have wider applications in fields like environmental remediation, catalysis, bio-medical and supercapacitance. Observations revealed that the MnO_2 and carbon micro- and nano-structured electrodes display exceptional performance in terms of electro-chemical factors and a capacitance per specific gravimetry of 454 Frigori at 0.051 mA/cm^2 of current density and capacitance maintenance of about 94% even beyond 6000 lifecycles. Manufacturing of magnetic carbon substrates having largely controlled morphology and properties and uniformly dispersed nano-structures were slightly complex. On contrast, in applications of optical imaging in which contrasting image method in inert nitrogen atmosphere spins with diamond is castoff and designed optimally rendered tremendous results.

Funding No funding received for this research.

Declarations

Conflict of interest The authors declare that they have no conflict of interest.

References

1. Chu H, Zhang Z, Liu Y, Leng J (2014) Self-heating fiber reinforced polymer composite using meso/macropore carbon nanotube paper and its application in deicing. Carbon 66:154–163
2. Anzar N, Hasan R, Tyagi M, Yadav N, Narang J (2020) Carbon nanotube—a review on synthesis, properties and plethora of applications in the field of biomedical science. Sensors Int 1:100003
3. Li J, Lu W, Suhr J, Chen H, Xiao JQ, Chou TW (2017) Superb electromagnetic wave-absorbing composites based on large-scale graphene and carbon nanotube films. Sci Rep 7(1):2349
4. Saravana Kumar A, Maivizhi Selvi P, Rajeshkumar L (2017) Delamination in drilling of sisal/banana reinforced composites produced by hand lay-up process. Appl Mech Mater 867:29–33
5. Yunlong Li, Wang Q, Wang S (2019) A review on enhancement of mechanical and tribological properties of polymer composites reinforced by carbon nanotubes and graphene sheet: molecular dynamics simulations. Compos B Eng 160:348–361
6. Yunlong Li, Wang S, Wang Q, Xing M (2018) A comparison study on mechanical properties of polymer composites reinforced by carbon nanotubes and graphene sheet. Compos B Eng 133:35–41
7. Nasouri K, Shoushtari AM (2017) Designing, modeling and manufacturing of lightweight carbon nanotubes/polymer composite nanofibers for electromagnetic interference shielding application. Compos Sci Technol 145:46–54
8. Zhu H, Wang X, Liang J, HonglingLv HT, Ma L, Yi Hu et al (2017) Versatile electronic skins for motion detection of joints enabled by aligned few-walled carbon nanotubes in flexible polymer composites. Adv Func Mater 27(21):1606604
9. El Moumen A, Tarfaoui M, Lafdi K (2017) Mechanical characterization of carbon nanotubes based polymer composites using indentation tests. Compos B Eng 114:1–7
10. Sweeney CB, Blake AL, Martin JP, Thomas CA, Victoria KH, Aaron GM, Blake RT, Mohammad AS, Micah JG (2017) Welding of 3D-printed carbon nanotube–polymer composites by locally induced microwave heating. Sci Adv 3(6):1700262

11. Tarfaoui M, El Moumen A, Lafdi K (2017) Progressive damage modeling in carbon fibers/carbon nanotubes reinforced polymer composites. Compos B Eng 112:185–195
12. Zhang L-Q, Yang B, Teng J, Lei J, Yan D-X, Zhong G-J, Li Z-M (2017) Tunable electromagnetic interference shielding effectiveness via multilayer assembly of regenerated cellulose as a supporting substrate and carbon nanotubes/polymer as a functional layer. J Mater Chem C 5(12):3130–3138
13. Ramesh M (2016) Kenaf (*Hibiscus cannabinus* L.) fibre based bio-materials: a review on processing and properties. Prog Mater Sci 78–79:1–92
14. Zhang L, De Greef N, Kalinka G, Van Bilzen B, Locquet J-P, IgnaasSeo VJW (2017) Carbon nanotube-grafted carbon fiber polymer composites: damage characterization on the micro-scale. Compos B Eng 126:202–210
15. Chaudhry MS, Czekanski A, Zhu ZH (2017) Characterization of carbon nanotube enhanced interlaminar fracture toughness of woven carbon fiber reinforced polymer composites. Int J Mech Sci 131:480–489
16. Chen J, Cui X, Zhu Y, Jiang W, Sui K (2017) Design of superior conductive polymer composite with precisely controlling carbon nanotubes at the interface of a co-continuous polymer blend via a balance of π-π interactions and dipole-dipole interactions. Carbon 114:441–448
17. Lebedev SM, Gefle OS, Amitov ET, Yu Berchuk D, Zhuravlev DV (2017) Poly (lactic acid)-based polymer composites with high electric and thermal conductivity and their characterization. Polym Testing 58:241–248
18. Cha J, Seongwoo JK, R, Soon HH, (2019) Comparison to mechanical properties of epoxy nanocomposites reinforced by functionalized carbon nanotubes and graphene nanoplatelets. Compos Part B Eng 162:283–288
19. Che J, Kai Wu, Lin Y, Wang Ke, Qiang Fu (2017) Largely improved thermal conductivity of HDPE/expanded graphite/carbon nanotubes ternary composites via filler network-network synergy. Compos A Appl Sci Manuf 99:32–40
20. Mora A, Han F, Lubineau G (2018) Estimating and understanding the efficiency of nanoparticles in enhancing the conductivity of carbon nanotube/polymer composites. Results Phys 10:81–90
21. Zhou B, Luo W, Yang J, XianbaoDuan YW, Zhou H, Chen R, Shan B (2017) Simulation of dispersion and alignment of carbon nanotubes in polymer flow using dissipative particle dynamics. Comput Mater Sci 126:35–42
22. El Moumen A, Tarfaoui M, Lafdi K, Benyahia H (2017) Dynamic properties of carbon nanotubes reinforced carbon fibers/epoxy textile composites under low-velocity impact. Compos Part B Eng 125:1–8
23. Sankaran S, Kalim Deshmukh M, Basheer Ahamed SK, Pasha K (2018) Recent advances in electromagnetic interference shielding properties of metal and carbon filler reinforced flexible polymer composites: a review. Compos A Appl Sci Manuf 114:49–71
24. Zhang H, Zhang G, Tang M, Zhou L, Li J, Fan X, Shi X, Qin J (2018) Synergistic effect of carbon nanotube and graphene nanoplates on the mechanical, electrical and electromagnetic interference shielding properties of polymer composites and polymer composite foams. Chem Eng J 353:381–393
25. Li Y, Huang X, Zeng L, Li R, Tian H, Xuewei Fu, Wang Yu, Zhong W-H (2019) A review of the electrical and mechanical properties of carbon nano filler-reinforced polymer composites. J Mater Sci 54(2):1036–1076
26. Wang J, Fang Z, AijuanGu LX, Liu Fu (2006) Effect of amino-functionalization of multi-walled carbon nanotubes on the dispersion with epoxy resin matrix. J Appl Polym Sci 100(1):97–104
27. Srivastava VK, Gries T, Veit D, Quadflieg T, Mohr B, Kolloch M (2017) Effect of nanomaterial on mode I and mode II interlaminar fracture toughness of woven carbon fabric reinforced polymer composites. Eng Fract Mech 180:73–86
28. Avilés F, Oliva-Avilés AI, Cen-Puc M (2018) Piezoresistivity, strain, and damage self-sensing of polymer composites filled with carbon nanostructures. Adv Eng Mater 20(7):1701159
29. Wang L, Liu Y, Zhang Z, Wang B, JingjingQiu DH, Wang S (2017) Polymer composites-based thermoelectric materials and devices. Compos B Eng 122:145–155
30. Li SQ, Wang F, Wang Ye, Wang JW, Ma J, Xiao J (2008) Effect of acid and TETA modification on mechanical properties of MWCNTs/epoxy composites. J Mater Sci 43(8):2653–2658
31. Radzuan NA, Mohd MY, Zakaria AB, Sulong JS (2017) The effect of milled carbon fibre filler on electrical conductivity in highly conductive polymer composites. Compos B Eng 110:153–160
32. Kinloch IA, Suhr J, Lou J, Young RJ, Ajayan PM (2018) Composites with carbon nanotubes and graphene: an outlook. Science 362(6414):547–553
33. Bhuvaneswari V, Rajeshkumar L, Balaji D, Saravanakumar R (2020) Study of mechanical and tribological properties of bioceramics reinforced aluminium alloy composites. Solid State Technol 63(5):4552–4560
34. Ma PC, Tang BZ, Kim J-K (2008) Effect of CNT decoration with silver nanoparticles on electrical conductivity of CNT-polymer composites. Carbon 46(11):1497–1505
35. Ramesh M, Arivumani R (2020) Carbon nanotube-based metal-organic framework nanocomposites. In: Metal-Organic Framework Nanocomposites. CRC Press, pp 237–260
36. Špitalský Z, Krontiras CA, Georga SN, Galiotis C (2009) Effect of oxidation treatment of multiwalled carbon nanotubes on the mechanical and electrical properties of their epoxy composites. Compos A Appl Sci Manuf 40(6–7):778–783
37. Kim YJ, Shin TS, Choi HD, Kwon JH, Chung Y-C, Yoon HoGyu (2005) Electrical conductivity of chemically modified multiwalled carbon nanotube/epoxy composites. Carbon 43(1):23–30
38. Jeong J-Y, Lee H-J, Kang S-W, Tan L-S, Baek J-B (2008) Nylon 610/functionalized multiwalled carbon nanotube composite prepared from in-situ interfacial polymerization. J Polym Sci Part A Polym Chem 46(18):6041–6050
39. Shi Y-D, Lei M, Chen Y-F, Zhang K, Zeng J-B, Wang M (2017) Ultralow percolation threshold in poly (l-lactide)/poly (ε-caprolactone)/multiwall carbon nanotubes composites with a segregated electrically conductive network. J Phys Chem C 121(5):3087–3098
40. Al-Saleh MH (2017) Clay/carbon nanotube hybrid mixture to reduce the electrical percolation threshold of polymer nanocomposites. Compos Sci Technol 149:34–40
41. Ramesh M, ArunRamnath R, Anish K, Aftab APK, Abdullah MA (2020) Electrically conductive self-healing materials: preparation, properties, and applications. In: Self-healing composite materials. Woodhead Publishing, pp 1–13. https://doi.org/10.1016/B978-0-12-817354-1.00001-6
42. Tang Z, Tang CH, Gong H (2012) A High energy density asymmetric supercapacitor from nano-architectured $Ni(OH)_2$/Carbon nanotube electrodes. Adv Funct Mater 22(6):1272–1278
43. Guo Z et al (2007) Flexible high-loading particle-reinforced polyurethane magnetic anocomposite fabrication through particle-surface-initiated polymerization. Nanotechnology 18(33):335704
44. Wang S et al (2015) Removal of arsenic by magnetic biochar prepared from pinewood and natural hematite. Biores Technol 175:391–395
45. Ramesh M, Deepa C (2019) Processing of green composites. Green Composites. Springer, Singapore, pp 47–72
46. Yu L et al (2009) Catalytic synthesis of carbon nanofibers and nanotubes by the pyrolysis of acetylene with iron nanoparticles

prepared using a hydrogen-arc plasma method. Mater Lett 63(20):1677–1679
47. Chiu W et al (2007) One pot synthesis of monodisperse Fe_3O_4 nanocrystals by pyrolysis reaction of organometallic compound. Mater Chem Phys 106(2):231–235
48. Ramesh M, Rajeshkumar L (2018) Wood flour filled thermoset composites. Materials Research Forum LLC. https://doi.org/10.21741/9781945291876-2
49. Shen Y, Yoshikawa K (2014) Tar conversion and vapour upgrading via in situ catalysis using silica-based nickel nanoparticles embedded in rice husk char for biomass pyrolysis/gasification. Ind Eng Chem Res 53(27):10929–10942
50. Liu X-M, Yang G, Fu S-Y (2007) Mass synthesis of nanocrystalline spinel ferrites by a polymer-pyrolysis route. Mater Sci Eng, C 27(4):750–755
51. Gong J et al (2013) Catalytic conversion of linear low density polyethylene into carbon nanomaterials under the combined catalysis of Ni_2O_3 and poly (vinyl chloride). Chem Eng J 215:339–347
52. Chen D-H, Liao M-H (2002) Preparation and characterization of YADH-bound magnetic nanoparticles. J Mol Catal B Enzym 16(5):283–291
53. Chi Y et al (2012) Synthesis of Fe_3O_4@ SiO_2–Ag magnetic nanocomposite based on small-sized and highly dispersed silver nanoparticles for catalytic reduction of 4-nitrophenol. J Colloid Interface Sci 383(1):96–102
54. Siddiqui M et al (2019) Characterization and process optimization of biochar produced using novel biomass, waste pomegranate peel: a response surface methodology approach. Waste Biomass Valoriz 10:521–532
55. Siddiqui M et al (2018) Thermogravimetric pyrolysis for neem char using novel agricultural waste: a study of process optimization and statistical modeling. Biomass Convers Biorefinery 8:857–871
56. Bradbury WLEAO (2011) Synthesis of carbide nanostructures on monolithic agricultural-waste biomass-activated carbon templates. Int J Appl Ceram Technol 8(4):947–952
57. Tan X et al (2015) Application of biochar for the removal of pollutants from aqueous solutions. Chemosphere 125:70–85
58. An SJ, Li J, Daniel C, Mohanty D, Nagpure S, Wood DL (2016) The state of understanding of the lithium-ion-battery graphite solid electrolyte interphase (SEI) and its relationship to formation cycling. Carbon 105:52–76
59. Ramesh M, Logesh R, Manikandan M, Sathesh Kumar N, Vishnu DP (2017) Mechanical and water intake properties of banana-carbon hybrid fiber reinforced polymer composites. Mater Res 20(2):365–376
60. Li F-S, Wu Y-S, Chou J, Winter M, Wu N-L (2015) A mechanically robust and highly ion-conductive polymer-blend coating for high-power and long-life lithium-ion battery anodes. Adv Mater 27:130–137
61. Song G, Ryu J, Ko S, Bang BM, Choi S, Shin Y, Lee S-Y (2016) Revisiting surface modification of graphite: dual-layer coating for high-performance lithium battery anode materials. Chem-An Asian J 11(11):1711–1717
62. Son S-B, Cao L, Yoon T, Cresce A, Hafner SE, Liu J, Groner M, Xu K, Ban C (2019) Interfacially induced cascading failure in graphite-silicon composite anodes. Adv Sci 6(3):1801007
63. De Arco LG, Zhang Y, Schlenker CW, Ryu K, Thompson ME, Zhou CW (2010) Continuous, highly flexible, and transparent graphene films by chemical vapour deposition for organic photovoltaics. ACS Nano 4(5):2865–2873
64. Zhang Y, Gomez L, Ishikawa FN, Madaria A, Ryu K, Wang CA, Badmaev A, Zhou CW (2010) Comparison of graphene growth on single-crystalline and polycrystalline Ni by chemical vapour deposition. J Phys Chem Lett 1(20):3101–3107
65. Karabacak T, Guclu H, Yuksel M (2009) Network behavior in thin film growth dynamics. Phys Rev B. https://doi.org/10.1103/PhysRevB.79.195418
66. Ramesh M, Bhoopathi R, Deepa C, Sasikala G (2018) Experimental investigation on morphological, physical and shear properties of hybrid composite laminates reinforced with flax and carbon fibers. J Chin Adv Mater Soc 6(4):640–654
67. Teng C-C, Ma C-C, Chu-Hua Lu, Yang S-Y, Lee S-H, Hsiao M-C, Yen M-Y, Chiou K-C, Lee T-M (2011) Thermal conductivity and structure of non-covalent functionalized graphene/epoxy composites. Carbon 49(15):5107–5116
68. Wan Y, Tang L, Gong L, Yan D, Li Y, Wu L, Jiang J, Lai G (2014) Grafting of epoxy chains onto graphene oxide for epoxy composites with improved mechanical and thermal properties. Carbon 69:467–480
69. Qian R, Jinhong Yu, Chao Wu, Zhai X, Jiang P (2013) Alumina-coated graphene sheet hybrids for electrically insulating polymer composites with high thermal conductivity. RSC Adv 3(38):17373–17379
70. Sun R, Yao H, Zhang H-B, Li Y, Mai Y-W, Zhong-Zhen Yu (2016) Decoration of defect-free graphene nanoplatelets with alumina for thermally conductive and electrically insulating epoxy composites. Compos Sci Technol 137:16–23
71. Zong P, Jifang Fu, Chen L, Yin J, Dong X, Yuan S, Shi L, Deng W (2016) Effect of aminopropylisobutyl polyhedral oligomeric silsesquioxane functionalized graphene on the thermal conductivity and electrical insulation properties of epoxy composites. RSC Adv 6(13):10498–10506
72. Ma W-S, Li Wu, Yang F, Wang S-F (2014) Non-covalently modified reduced graphene oxide/polyurethane nanocomposites with good mechanical and thermal properties. J Mater Sci 49(2):562–571
73. Varenik M, Nadiv R, Levy I, Vasilyev G, Regev O (2017) Breaking through the solid/liquid processability barrier: thermal conductivity and rheology in hybrid graphene–graphite polymer composites. ACS Appl Mater Interfaces 9(8):7556–7564
74. Li An, Zhang C, Zhang Y-F (2017) RGO/TPU composite with a segregated structure as thermal interface material. Compos A Appl Sci Manuf 101:108–114
75. Tian L, Wang Y, Li Z, Mei H, Shang Y (2017) The thermal conductivity-dependant drag reduction mechanism of water droplets controlled by graphene/silicone rubber composites. Exp Thermal Fluid Sci 85:363–369
76. Balaji D, Ramesh M, Kannan T, Deepan S, Bhuvaneswari V, Rajeshkumar L (2020) Experimental investigation on mechanical properties of banana/snake grass fiber reinforced hybrid composites. Mater Today Proc. https://doi.org/10.1016/j.matpr.2020.09.548
77. Alam FE, Dai W, Yang M, Shiyu Du, Li X, Jinhong Yu, Jiang N, Lin C-T (2017) In situ formation of a cellular graphene framework in thermoplastic composites leading to superior thermal conductivity. J Mater Chem A 5(13):6164–6169
78. Yan H, Tang Y, Long W, Li Y (2014) Enhanced thermal conductivity in polymer composites with aligned graphene nanosheets. J Mater Sci 49(15):5256–5264
79. Wu K, Lei C, Huang R, Yang W, Chai S, Geng C, Chen F, Qiang Fu (2017) Design and preparation of a unique segregated double network with excellent thermal conductive property. ACS Appl Mater Interfaces 9(8):7637–7647
80. Ryu J, Kim Y, Won D, Kim N, Park JS, Lee EK, Cho D, Cho SP, Kim SJ, Ryu GH, Shin HAS, Lee Z, Hong BH, Cho S (2014) Fast synthesis of high-performance graphene films by hydrogen-free rapid thermal chemical vapour deposition. ACS Nano 8(1):950–956

81. Ramesh M, Rajesh Kumar L, Anish K, Abdullah MA (2020) Self-healing polymer composites and its chemistry. In: Self-healing composite materials. Woodhead Publishing, pp 415–427
82. Wang F, Yi J, Wang Y, Wang C, Wang J, Xia Y (2014) Graphite intercalation compounds (GICs): a new type of promising anode material for lithium-ion batteries. Adv Energy Mater 4(2):1300600
83. Vissers DR, Chen Z, Shao Y, Engelhard M, Das U, Redfern P, Curtiss LA, Pan B, Liu J, Amine K (2016) Role of Manganese deposition on graphite in the capacity fading of lithium ion batteries. ACS Appl Mater Interfaces 8(22):14244–14251
84. Chang C-C, Liu S-J, Wu J-J, Yang C-H (2007) Nano-tin Oxide/Tin particles on a graphite surface as an anode material for lithium-ion batteries. J Phys Chem C 111(44):16423–16427
85. Cao X, Li Y, Li X, Zheng J, Gao J, Gao Y, Wu X, Zhao Y, Yang Y (2013) Novel phosphamide additive to improve thermal stability of solid electrolyte interphase on graphite anode in lithium-ion batteries. ACS Appl Mater Interfaces 5(22):11494–11497
86. Ramesh M, ArunRamnath R, Deepa C (2021) Friction and wear properties of carbon nanotube-reinforced polymer composites. In: Tribology of polymer composites: characterization, properties, and applications, pp 223–240
87. Jiang S, Sun F, Fan H, Fang D (2017) Fabrication and testing of composite orthogrid sandwich cylinder. Compos Sci Technol 142:171–179
88. Wu SR, Chen TH, Tsai HY (2019) A review of actuation force in origami applications. J Mech 35(5):627–639
89. Gattas JM, You Z (2015) The behaviour of curved-crease origami foldcores under low-velocity impact loads. Int J Solids Struct 53:80–91
90. Schenk M, Guest SD, McShane GJ (2014) Novel stacked folded cores for blast-resistant sandwich beams. Int J Solids Struct 51:4196–4214
91. Kintscher M, Kärger L, Wetzel A, Hartung D (2007) Stiffness and failure behaviour of folded sandwich cores under combined transverse shear and compression. Compos Part A 38:1288–1295
92. Ramesh M, Deepa C, Tamil Selvan M, Hemachandra Reddy K (2020) Effect of alkalization on characterization of ripe bulrush (Typha Domingensis) grass fiber reinforced epoxy composites. J Nat Fibers. https://doi.org/10.1080/15440478.2020.1764443
93. Demiral M, Kadioglu F (2018) Failure behaviour of the adhesive layer and angle ply composite adherends in single lap joints: a numerical study. Int J Adhes Adhes 87:181–190
94. Le Q-H, Kuan H-C, Dai J-B, Zaman I, Luong L, Ma J (2010) Structure–property relations of 55 nm particle-toughened epoxy. Polymer 51(21):4867–4879
95. Difallah BB, Kharrat M, Dammak M, Monteil G (2012) Microstructure, friction and wear analysis of thermoplastic based composites with solid lubricant. Mech Ind 13(5):337–346
96. Ma J, Mo MS, Du XS, Dai SR, Luck I (2008) Study of epoxy toughened by in situ formed rubber nanoparticles. J Appl Polym Sci 110(1):304–312
97. Kuan HC, Dai JB, Ma J (2010) A reactive polymer for toughening epoxy resin. J Appl Polym Sci 115(6):3265–3272
98. Maschio G, Koufopanos C, Lucchesi A (1992) Pyrolysis, a promising route for biomass utilization. Biores Technol 42(3):219–231
99. Harris K et al (2013) Characterization and mineralization rates of low temperature peanut hull and pine chip biochars. Agronomy 3(2):294–312
100. Goyal H, Seal D, Saxena R (2008) Bio-fuels from thermo-chemical conversion of renewable resources: a review. Renew Sustain Energy Rev 12(2):504–517
101. Ramesh M, Deepa C, Tamil Selvan M, Rajeshkumar L, Balaji D, Bhuvaneswari V (2020) Mechanical and water absorption properties of *Calotropis gigantea* plant fibers reinforced polymer composites. Mater Today Proc. https://doi.org/10.1016/j.matpr.2020.11.480
102. Wang L et al (2009) Technical and economical analyses of combined heat and power generation from distillers grains and corn stover in ethanol plants. Energy Convers Manag 50(7):1704–1713
103. Saunders J, Rosentrater K (2009) Properties of solvent extracted low-oil corn distillers dried grains with solubles. Biomass Bioenerg 33(10):1486–1490
104. McKendry P (2002) Energy production from biomass (part 2): conversion technologies. Biores Technol 83(1):47–54
105. Thines K et al (2017) Synthesis of magnetic biochar from agricultural waste biomass to enhancing route for waste water and polymer application: a review. Renew Sustain Energy Rev 67:257–276
106. Fan L-W, Zhu Z-Q, Zeng Yi, Qian Lu, Zi-Tao Yu (2014) Heat transfer during melting of graphene-based composite phase change materials heated from below. Int J Heat Mass Transf 79:94–104
107. Shi L, Wang Y, Ding S, Zhenyu Chu Yu, Yin DJ, Luo J, Jin W (2017) A facile and green strategy for preparing newly-designed 3D graphene/gold film and its application in highly efficient electrochemical mercury assay. Biosens Bioelectron 89:871–879
108. Li B, Dong S, Xuan Wu, Wang C, Wang X, Fang J (2017) Anisotropic thermal property of magnetically oriented carbon nanotube/graphene polymer composites. Compos Sci Technol 147:52–61
109. Dongn HS, Qi SJ (2015) Realising the potential of graphene-based materials for biosurfaces – A future perspective. Biosurface and Biotribology 1:229–248
110. Urbanová V, Bakandritsos A, Jakubec P, Szambó T, Zbořila R (2017) A facile graphene oxide based sensor for electrochemical detection of neonicotinoids. Biosens Bioelectron 89:532–537
111. Liu X-G, Xing X-J, Li Bo, Guo Y-M, Zhang Y-Z, Yang Y, Zhang L-F (2016) Fluorescent assay for alkaline phosphatase activity based on graphene oxide integrating with λ exonuclease. Biosens Bioelectron 81:460–464
112. Lee S-W, Choi BI, Kim JC, Woo S-B, Kim Y-G, Kwon S, Yoo J, Seo Y-S (2016) Sorption/desorption hysteresis of thin-film humidity sensors based on graphene oxide and its derivative. Sens Actuators B Chem 237:575–580
113. Sun A-L, Zhang Y-F, Sun G-P, Wang X-N, Tang D (2017) Homogeneous electrochemical detection of ochratoxin A in foodstuff using aptamer–graphene oxide nanosheets and DNase I-based target recycling reaction. Biosens Bioelectron 89:659–665
114. Liu Q, Guo-Rong Xu (2016) Graphene oxide (GO) as functional material in tailoring polyamide thin film composite (PA-TFC) reverse osmosis (RO) membranes. Desalination 394:162–175
115. Sarker PC, Masud Rana Md, Sarkar AK (2017) A simple FDTD approach for the analysis and design of graphene based optical devices. Optik 144:1–8
116. Zeyu Lu, Li X, Hanif A, Chen B, Parthasarathy P, Jinguang Yu, Li Z (2017) Early-age interaction mechanism between the graphene oxide and cement hydrates. Constr Build Mater 152:232–239
117. Cao R, Liu H, Chen S, Pei D, Miao J, Zhang X (2017) Fabrication and properties of graphene oxide-grafted-poly(hexadecylacrylate) as a solid-solid phase change material. Compos Sci Technol 149:262–268
118. Sturm R, Klett Y, Kindervater C, Voggenreiter H (2014) Failure of CFRP airframe sandwich panels under crash-relevant loading conditions. Compos Struct 112:11–21
119. Gattas JM, You Z (2014) Quasi-static impact of indented foldcores. Int J Impact Eng 73:15–29

120. Ramesh M, Rajesh Kumar L, Bhuvaneshwari V (2020) Bamboo fiber reinforced composites. Bamboo Fiber Composites. Springer, Singapore, pp 1–13
121. Lebée KS (2010) Transverse shear stiffness of a chevron folded core used in sandwich construction. Int J Solids Struct 47:2620–2629
122. Boatti E, Vasios N, Bertoldi K (2017) origami metamaterials for tunable thermal expansion. Adv Mater 29:1700360
123. Pratapa PP, Suryanarayana P, Paulino GH (2018) Bloch wave framework for structures with nonlocal interactions: application to the design of origami acoustic metamaterials. J Mech Phys Solids 118:115–132
124. Gattas JM, You Z (2014) Miura-base rigid origami: parametrizations of curved-crease geometries. J. Mech. Design 136:121404
125. Tolley MT, Samuel MF, Shuhei M, Daniel A, Daniela R, Robert JW (2014) Self-folding origami: shape memory composites activated by uniform heating. Smart Mater Struct 23(9):094006
126. Miyashita S, Isabella DD, Ishwarya A, Byoungkwon A, Cynthia S, Slava A, Daniela R (2015) Folding angle regulation by curved crease design for self-assembling origami propellers. J Mech Robot 7(2):021013
127. Han B, Zhang Z, Zhang Q, Zhang Q, Lu TJ, Lu B (2017) Recent advances in hybrid lattice-cored sandwiches for enhanced multifunctional performance. Extreme Mech Lett 10:58–69
128. Shigemune H, Maeda S, Hara Y, Hosoya N, Hashimoto S (2016) Origami robot: a self-folding paper robot with an electro-thermal actuator created by printing. IEEE/ASME Trans Mechatron 21(6):2746–2754
129. Gattas JM, Wu W, You Z (2013) Miura-base rigid origami: parameterizations of first-level derivative and piecewise geometries. J Mech Design 135:111011
130. Fischer S, Drechsler K, Kilchert S, Johnson A (2009) Mechanical tests for foldcore base material properties. Compos Part A 40:1941–1952
131. Fischer S (2015) Aluminium foldcores for sandwich structure application: mechanical properties and FE-simulation. Thin Wall Struct 90:31–41
132. Ramesh M, Deepa C, Arpitha GR, Gopinath V (2019) Effect of hybridization on properties of hemp-carbon fibre-reinforced hybrid polymer composites using experimental and finite element analysis. World J Eng 16(2):248–259
133. Sun Y, Li Y (2017) Prediction and experiment on the compressive property of the sandwich structure with a chevron carbon-fibre-reinforced composite folded core. Compos Sci Technol 150:95–101
134. Prabhu L, Krishnaraj V, Gokulkumar S, Sathish S, Sanjay MR, Siengchin S (2020) Mechanical, chemical and sound absorption properties of glass/kenaf/waste tea leaf fiber-reinforced hybrid epoxy composites. J Ind Text. https://doi.org/10.1177/1528083720957392
135. Heimbs S, Cichosz J, Klaus M, Kilchert S, Johnson AF (2010) Sandwich structures with textile-reinforced composite foldcores under impact loads. Compos Struct 92:1485–1497
136. Alekseev KA, Zakirov IM, Karimova GG (2011) Geometrical model of creasing roll for manufacturing line of the wedge-shaped folded cores production. Russ Aeronaut 54:104–107
137. Ramesh M, Rajesh Kumar L (2020) Bioadhesives. Green Adhesives: Preparation, Properties and Applications, pp 145–164. https://doi.org/10.1002/9781119655053.ch7
138. Morgan J, Spencer PM, Larry LH (2016) An approach to designing origami-adapted aerospace mechanisms. J Mech Des 10(1115/1):4032973
139. Paez L, Agarwal G, Paik J (2016) Design and analysis of a soft pneumatic actuator with origami shell reinforcement. Soft Rob 3(3):109–119
140. Vazifehdoostsaleh A, Fatouraee N, Navidbakhsh M, Izadi F (2018) Three dimensional FSI modelling of sulcus vocalis disorders of vocal folds. J Mech 34(6):791–800
141. Vazifehdoostsaleh A, Fatouraee N, Navidbakhsh M, Izadi F (2017) Numerical analysis of the sulcus vocalis disorder on the function of the vocal folds. J Mech 33(4):513–520
142. L. LaRue, B.B. Basily, E.A. Elsayed. 2009. Cushioning systems for impact energy absorption. http://www.ise.rutgers.edu/research/working_paper/paper%2004-016.pdf
143. Zhou X, Wang H, You Z (2014) Mechanical properties of Miura-based folded cores under quasi-static loads. Thin Wall Struct 82:296–310
144. Zhou J-H, Sui Z-J, Zhu J, Li P, Chen D, Dai Y-C, Yuan W-K (2007) Characterization of surface oxygen complexes on carbon nanofibers by TPD. XPS and FT-IR Carbon 45(4):785–796
145. Ramesh M (2018) Hemp, jute, banana, kenaf, ramie, sisal fibers. In Handbook of Properties of Textile and Technical Fibres. Woodhead Publishing, pp 301–325
146. Thomas S Spectroscopic Tools. http://www.science-and-fun.de/tools/
147. Xu Y, Zhang C, Zhou M, Qun Fu, Zhao C, Minghong Wu, Lei Y (2018) Highly nitrogen doped carbon nanofibers with superior rate capability and cyclability for potassium ion batteries. Nat Commun 9(1):1–11
148. Cipriani E, Zanetti M, Bracco P, Brunella V, Luda MP, Costa L (2016) Crosslinking and carbonization processes in PAN films and nanofibers. Polym Degrad Stab 123:178–188
149. Fang W, Yang S, Wang X-L, Yuan T-Q, Sun R-C (2017) Manufacture and application of lignin-based carbon fibers (LCFs) and lignin-based carbon nanofibers (LCNFs). Green Chem 19(8):1794–1827
150. Yin H, Hong-Qing Qu, Liu Z, Jiang R-Z, Li C, Zhu M-Q (2019) Long cycle life and high rate capability of three dimensional $CoSe_2$ grain-attached carbon nanofibers for flexible sodium-ion batteries. Nano Energy 58:715–723
151. Parveen S, Sohel R, Raul F (2013) A review on nanomaterial dispersion, microstructure, and mechanical properties of carbon nanotube and nanofiber reinforced cementitious composites. J Nanomater 2013:710175
152. Pels JR, Kapteijn F, Moulijn JA, Zhu Q, Thomas KM (1995) Evolution of nitrogen functionalities in carbonaceous materials during pyrolysis. Carbon 33(11):1641–1653
153. Wu M, Wang Y, Wei Z, Wang L, Zhuo M, Zhang J, Han X, Ma J (2018) Ternary doped porous carbon nanofibers with excellent ORR and OER performance for zinc–air batteries. J Mater Chem A 6(23):10918–10925
154. Titantah JT, Lamoen D (2007) Carbon and nitrogen 1s energy levels in amorphous carbon nitride systems: XPS interpretation using first-principles. Diam Relat Mater 16(3):581–588
155. Ramesh M, Deepa C, Rajesh Kumar L, Sanjay MR, Suchart S (2020) Life-cycle and environmental impact assessments on processing of plant fibres and its bio-composites: a critical review. J Ind Text. https://doi.org/10.1177/1528083720924730
156. Chen L-F, Yan Lu, Le Yu, Lou XWD (2017) Designed formation of hollow particle-based nitrogen-doped carbon nanofibers for high-performance supercapacitors. Energy Environ Sci 10(8):1777–1783
157. Wang C, Kaneti YV, Bando Y, Lin J, Liu C, Li J, Yamauchi Y (2018) Metal–organic framework-derived one-dimensional porous or hollow carbon-based nanofibers for energy storage and conversion. Mater Horiz 5(3):394–407
158. Hao R, HaoLan CK, Wang H, Guo L (2018) Superior potassium storage in chitin-derived natural nitrogen-doped carbon nanofibers. Carbon 128:224–230
159. Quan D, Urdaniz JL, Ivankovic A (2018) Enhancing mode-I and mode-II fracture toughness of epoxy and carbon fibre

reinforced epoxy composites using multi-walled carbon nanotubes. Mater Des 143:81–92
160. Domun N, Hadavinia H, Zhang T, Sainsbury T, Liaghat GH, Vahid S (2015) Improving the fracture toughness and the strength of epoxy using nanomaterials-a review of the current status. Nanoscale 7(23):10294–10329
161. Heidarinejad Z, Dehghani MH, Heidari M, Javedan G, Ali I, Sillanpää M (2020) Methods for preparation and activation of activated carbon: a review. Environ Chem Lett 18(2):393–415
162. Rocha LS, Pereira D, Sousa É, Otero M, Esteves VI, Calisto V (2020) Recent advances on the development and application of magnetic activated carbon and char for the removal of pharmaceutical compounds from waters: a review. Sci Total Environ 718:137272
163. Hassan MF, Sabri MA, Fazal H, Hafeez A, Shezad N, Hussain M (2020) Recent trends in activated carbon fibers production from various precursors and applications—a comparative review. J Anal Appl Pyrolysis 145:104715
164. Rahimian R, Zarinabadi S (2020) A review of studies on the removal of methylene blue dye from industrial wastewater using activated carbon adsorbents made from almond bark. Prog Chem Biochem Res 3(3):251–268
165. Anfar Z, Ait Ahsaine H, Zbair M, Amedlous A, Ait El Fakir A, Jada A, El Alem N (2020) Recent trends on numerical investigations of response surface methodology for pollutants adsorption onto activated carbon materials: a review. Crit Rev Environ Sci Technol 50(10):1043–1084
166. Reza MS, Yun CS, Afroze S, Radenahmad N, Bakar MSA, Saidur R, Taweekun J, Azad AK (2020) Preparation of activated carbon from biomass and its' applications in water and gas purification, a review. Arab J Basic Appl Sci 27(1):208–238
167. Ramesh M, Rajeshkumar L, Balaji D (2021) Aerogels for Insulation Applications. Aerogels II Prep Prop Appl 98:57–76
168. Fan Y, Fowler GD, Zhao M (2020) The past, present and future of carbon black as a rubber reinforcing filler–a review. J Clean Prod 247:119115
169. Junqing X, Jiaxue Y, Jianglin X, Chenliang S, Wenzhi H, Juwen H, Guangming L (2020) High-value utilization of waste tires: a review with focus on modified carbon black from pyrolysis. Sci Total Environ 140235
170. Khodabakhshi S, Fulvio PF, Andreoli E (2020) Carbon black reborn: structure and chemistry for renewable energy harnessing. Carbon 162:604–649
171. Szadkowski B, Marzec A, Zaborski M (2020) Use of carbon black as a reinforcing nano-filler in conductivity-reversible elastomer composites. Polym Testing 81:106222
172. Babu B (2008) Biomass pyrolysis: a state-of-the-art review. Biofuels Bioprod Biorefin 2(5):393–414
173. Roy C, Chaala A, Darmstadt H (1999) The vacuum pyrolysis of used tires: end-uses for oil and carbon black products. J Anal Appl Pyrol 51(1–2):201–221
174. González-Arias J, Marta ES, Elia JM, Camila C, Ana A-S, Rubén G, Jorge C-J (2020) Hydrothermal carbonization of olive tree pruning as a sustainable way for improving biomass energy potential. Effect of reaction parameters on fuel properties. Processes 8(10):1201
175. Li Z, Liu J, Jiang K, Thundat T (2016) Carbonized nanocellulose sustainably boosts the performance of activated carbon in ionic liquid supercapacitors. Nano Energy 25:161–169
176. Deng L, Young RJ, Kinloch IA, Abdelkader AM, Holmes SM, De Haro-Del DA, Rio SJ, Eichhorn. (2013) Supercapacitance from cellulose and carbon nanotube nanocomposite fibers. ACS Appl Mater Interfaces 5(20):9983–9990
177. Deng L, Zhong W, Wang J, Zhang P, Fang H, Yao L, Liu X, Ren X, Li Y (2017) The enhancement of electrochemical capacitance of biomass-carbon by pyrolysis of extracted nanofibers. ElectrochimicaActa 228:398–406
178. Lai C, Zhou Z, Zhang L, Wang X, Zhou Q, Zhao Y, Wang Y, Xiang-Fa Wu, Zhu Z, Fong H (2014) Free-standing and mechanically flexible mats consisting of electrospun carbon nanofibers made from a natural product of alkali lignin as binder-free electrodes for high-performance supercapacitors. J Power Sour 247:134–141
179. Bhuvaneswari V, Priyadharshini M, Deepa C, Balaji D, Rajeshkumar L, Ramesh M (2021) Deep learning for material synthesis and manufacturing systems: a review. Mater Today Proc. https://doi.org/10.1016/j.matpr.2020.11.351
180. Duan Bo, Xiang Gao Xu, Yao YF, Huang L, Zhou J, Zhang L (2016) Unique elastic N-doped carbon nanofibrous microspheres with hierarchical porosity derived from renewable chitin for high rate supercapacitors. Nano Energy 27:482–491
181. Yang Y, Chuchu C, Dagang L (2018) Electrodes based on cellulose nanofibers/carbon nanotubes networks, polyaniline nanowires and carbon cloth for supercapacitors. Mater Res Express 6(3):035008
182. Liu W-J, Tian Ke, He Y-R, Jiang H, Han-Qing Yu (2014) High-yield harvest of nanofibers/mesoporous carbon composite by pyrolysis of waste biomass and its application for high durability electrochemical energy storage. Environ Sci Technol 48(23):13951–13959
183. Mohan D, Kumar S, Srivastava A (2014) Fluoride removal from ground water using magnetic and nonmagnetic corn stoverbiochars. Ecol Eng 73:798–808
184. Shah DO (2002) Fine particles: Synthesis, characterization, and mechanisms of growth. Edited by T. Sugimoto, surfactant science series. J Nanopar Res 92(4):179. https://doi.org/10.1023/A:1020110320804
185. Shen Y et al (2009) Preparation and application of magnetic Fe_3O_4 nanoparticles for wastewater purification. Sep Purif Technol 68(3):312–319
186. Kolthoff I (1932) Theory of coprecipitation The formation and properties of crystalline precipitates. J Phys Chem 36(3):860–881
187. Jeong JR et al (2004) Magnetic properties of γ-Fe_2O_3 nanoparticles made by coprecipitation method. Phys Status Solidi (B) 241(7):1593–1596
188. Titirici MM, Thomas A, Antonietti M (2007) Replication and coating of silica templates by hydrothermal carbonization. Adv Func Mater 17(6):1010–1018
189. Manafi S, Nadali H, Irani H (2008) Low temperature synthesis of multi-walled carbon nanotubes via a sonochemical/hydrothermal method. Mater Lett 62(26):4175–4176
190. Titirici M-M, Thomas A, Antonietti M (2007) Back in the black: hydrothermal carbonization of plant material as an efficient chemical process to treat the CO_2 problem? New J Chem 31(6):787–789
191. Jamari SS, Howse JR (2012) The effect of the hydrothermal carbonization process on palm oil empty fruit bunch. Biomass Bioenergy 47:82–90
192. Liu Z, Zhang F-S, Wu J (2010) Characterization and application of chars produced from pinewood pyrolysis and hydrothermal treatment. Fuel 89(2):510–514
193. Sevilla M, Macia-Agullo JA, Fuertes AB (2011) Hydrothermal carbonization of biomass as a route for the sequestration of CO_2: chemical and structural properties of the carbonized products. Biomass Bioenergy 35(7):3152–3159
194. Xiao L-P et al (2012) Hydrothermal carbonization of lignocellulosic biomass. Biores Technol 118:619–623
195. Bobleter O (1994) Hydrothermal degradation of polymers derived from plants. Prog Polym Sci 19(5):797–841

196. Titirici M-M et al (2012) Black perspectives for a green future: hydrothermal carbons for environment protection and energy storage. Energy Environ Sci 5(5):6796–6822
197. Hu B et al (2010) Engineering carbon materials from the hydrothermal carbonization process of biomass. Adv Mater 22(7):813–828
198. Sevilla M, Fuertes AB (2009) Chemical and structural properties of carbonaceous products obtained by hydrothermal carbonization of saccharides. Chemistry-A European Journal 15(16):4195–4203
199. Wang Q et al (2001) Monodispersed hard carbon spherules with uniform nanopores. Carbon 39(14):2211–2214
200. Jain A, Balasubramanian R, Srinivasan M (2016) Hydrothermal conversion of biomass waste to activated carbon with high porosity: A review. Chem Eng J 283:789–805
201. Falco C et al (2013) Tailoring the porosity of chemically activated hydrothermal carbons: influence of the precursor and hydrothermal carbonization temperature. Carbon 62:346–355
202. Falco C, Baccile N, Titirici M-M (2011) Morphological and structural differences between glucose, cellulose and lignocellulosic biomass derived hydrothermal carbons. Green Chem 13(11):3273–3281
203. Cui X, Antonietti M, Yu SH (2006) Structural effects of iron oxide nanoparticles and iron ions on the hydrothermal carbonization of starch and rice carbohydrates. Small 2(6):756–759
204. Zhang S et al (2010) Preparation of carbon coated Fe_3O_4 nanoparticles and their application for solid-phase extraction of polycyclic aromatic hydrocarbons from environmental water samples. J Chromatogr A 1217(29):4757–4764
205. Lim YS, Lai CW, Hamid SBA (2017) Porous 3D carbon decorated Fe_3O_4 nanocomposite electrode for highly symmetrical supercapacitor performance. RSC Adv 7(37):23030–23040
206. Tang Z et al (2016) Enhanced removal of Pb (II) by supported nanoscale Ni/Fe on hydrochar derived from biogas residues. Chem Eng J 292:224–232
207. Titirici M-M, Antonietti M (2010) Chemistry and materials options of sustainable carbon materials made by hydrothermal carbonization. Chem Soc Rev 39(1):103–116
208. Tang L et al (2012) Deep ultraviolet photoluminescence of water-soluble self-passivated graphene quantum dots. ACS Nano 6(6):5102–5110
209. Zang S, Zhou X, Wang H, You Z (2016) Foldcores made of thermoplastic materials: experimental study and finite element analysis. Thin Wall Struct 100:170–179
210. Wang C, Zaouk R, Madou M (2006) Local chemical vapour deposition of carbon nanofibers from photoresist. Carbon 44:3073–3077
211. De Volder MF, Vansweevelt R, Wagner P, Reynaerts D, Van HC, Hart AJ (2011) Hierarchical carbon nanowire microarchitectures made by plasma-assisted pyrolysis of photoresist. ACS Nano 5:6593–6600
212. Thakur V, Singha A, Thakur M (2013) Synthesis of natural cellulose–based graft copolymers using methyl methacrylate as an efficient monomer. Adv Polym Technol 32(S1):E741–E748
213. Methner M et al (2010) Nanoparticle emission assessment technique (NEAT) for the identification and measurement of potential inhalation exposure to engineered nanomaterials—Part B: results from 12 field studies. J Occup Environ Hyg 7(3):163–176
214. Wu Z et al (2012) General and controllable synthesis of novel mesoporous magnetic iron oxide@carbon encapsulates for efficient arsenic removal. Adv Mater 24(4):485–491
215. Wang W et al (2012) The use of graphene-based magnetic nanoparticles as adsorbent for the extraction of triazole fungicides from environmental water. J Sep Sci 35(17):2266–2272
216. Xia H, Lai M, Lu L (2010) Nanoflaky MnO_2/carbon nanotube nanocomposites as anode materials for lithium-ion batteries. J Mater Chem 20:6896–6902
217. Oliveira LC et al (2002) Activated carbon/iron oxide magnetic composites for the adsorption of contaminants in water. Carbon 40(12):2177–2183
218. Suri K et al (2002) Gas and humidity sensors based on iron oxide–polypyrrole nanocomposites. Sens Actuators B Chem 81(2–3):277–282
219. Xie J et al (2011) Surface-engineered magnetic nanoparticle platforms for cancer imaging and therapy. Acc Chem Res 44(10):883–892
220. Zhi M et al (2013) Nanostructured carbon–metal oxide composite electrodes for supercapacitors: a review. Nanoscale 5(1):72–88
221. Chen Y et al (2012) Synthesis of porous hollow Fe_3O_4 beads and their applications in lithium ion batteries. J Mater Chem 22(11):5006–5012
222. Daniel ED, Levine I (1960) Experimental and theoretical investigation of the magnetic properties of iron oxide recording tape. J Acoust Soc Am 32(1):1–15
223. Quan H et al (2016) One-pot synthesis of α-Fe_2O_3nanoplates-reduced graphene oxide composites for supercapacitor application. Chem Eng J 286:165–173
224. Zhang C, Li Y, Wang P, Zhang H (2020) Electrospinning of nanofibers: potentials and perspectives for active food packaging. Compr Rev Food Sci Food Saf 19(2):479–502
225. Zhu X et al (2014) Novel and high-performance magnetic carbon composite prepared from waste hydrochar for dye removal. ACS Sustain Chem Eng 2(4):969–977
226. Cao F et al (2009) 3D Fe_3S_4 flower-like microspheres: high-yield synthesis via a biomolecule assisted solution approach, their electrical, magnetic and electrochemical hydrogen storage properties. Dalton Trans 42:9246–9252
227. Berry CC, Curtis AS (2003) Functionalisation of magnetic nanoparticles for applications in biomedicine. J Phys D Appl Phys 36(13):R198–R206
228. Lok C (2001) Picture perfect. Nature 412(6845):372–375
229. Ramesh M, Rajeshkumar L, Balaji D, Bhuvaneswari V (2021) Green composite using agricultural waste reinforcement. In: Thomas S, Balakrishnan P (eds) Green composites. Materials horizons: from nature to nanomaterials. Springer, Singapore. https://doi.org/10.1007/978-981-15-9643-8_2
230. Halavaara J et al (2002) Efficacy of sequential use of superparamagnetic iron oxide and gadolinium in liver MR imaging. Acta Radiol 43(2):180–185
231. Dobson J (2006) Gene therapy progress and prospects: magnetic nanoparticle-based gene delivery. Gene Ther 13(4):283–287
232. Barcena C, Sra AK, Gao J (2009) Applications of magnetic nanoparticles in biomedicine. Nanoscale magnetic materials and applications. Springer, New York, pp 591–626
233. Wang SX, Li G (2008) Advances in giant magnetoresistance biosensors with magnetic nanoparticle tags: review and outlook. IEEE Trans Magn 44(7):1687–1702